

Title: Haspin Kinase Has Multiple Functions In The Plant Cell Division Regulatory Network

Running title: Haspin kinase in plant cell division

Corresponding author: Daisuke Kurihara

Division of Biological Science, Graduate School of Science, Nagoya University, Furo-cho,
Chikusa-ku, Nagoya, Aichi 464-8602, Japan

Higashiyama Live-Holonics Project, ERATO, JST, Furo-cho, Chikusa-ku, Nagoya, Aichi
464-8602, Japan

Tel: +81-52-789-2496

Fax: +81-52-789-2497

E-mail: kuri@bio.nagoya-u.ac.jp

Subject areas: Growth and development, Structure and function of cells

Number of black and white figures: 2

Number of color figures: 5

Number of tables: 0

Supplementary materials: 8

Title: Haspin kinase has multiple functions in the plant cell division regulatory network

Running title: Haspin kinase in plant cell division

Authors: Elena Kozgunova¹, Takamasa Suzuki^{2,3}, Masaki Ito^{4,5}, Tetsuya Higashiyama^{1,3,6},
Daisuke Kurihara^{1,3,*}

Affiliations:

¹Division of Biological Science, Graduate School of Science, Nagoya University, Furo-cho, Chikusa-ku, Nagoya, Aichi 464-8602, Japan

²College of Bioscience and Biotechnology, Chubu University, Matsumoto-cho, Kasugai, Aichi 478-8501, Japan

³Higashiyama Live-Holonics Project, ERATO, JST, Furo-cho, Chikusa-ku, Nagoya, Aichi 464-8602, Japan

⁴Division of Biological Science, Graduate School of Bioagricultural Sciences, Nagoya University, Furo-cho, Chikusa-ku, Nagoya, Aichi 464-8601, Japan

⁵JST, CREST, Furo-cho, Chikusa-ku, Nagoya, Aichi 464-8601, Japan

⁶Institute of Transformative Bio-Molecules (ITbM), Nagoya University, Furo-cho, Chikusa-ku, Nagoya, Aichi 464-8602, Japan

Abbreviations: 5-ITu, 5-Iodotubercidin; ANOVA, analysis of variance; AUR1, Aurora1 kinase; AUR2, Aurora2 kinase; AUR3, Aurora3 kinase; BY-2, Bright Yellow-2; CenH3, centromeric histone H3; CPC, chromosome passenger complex; DMSO, dimethyl sulfoxide; GFP, green fluorescent protein; GST, glutathione S-transferase; H3S10ph, phosphorylation of histone H3 at serine10; H3S28ph, phosphorylation of histone H3 at serine28; H3T11ph, phosphorylation of histone H3 at threonine11; H3T3ph, phosphorylation of histone H3 at threonine3; MAP65,

microtubule-associated protein 65; MT, microtubules; NEBD, nuclear envelope breakdown; tdTomato, tandem dimer Tomato.

Footnotes: The nucleotide sequences reported in this paper have been submitted to the DDBJ/EMBL/GenBank databases under the following accession numbers: LC052296, (NtHaspin), LC052297 (NtAUR1), LC052298 (NtAUR2), and LC052299 (NtAUR3).

Abstract

Progression of the cell division is controlled by a various mitotic kinases. In animal cells, phosphorylation of histone H3 at Thr3 by Haspin kinase promotes centromeric Aurora B localization to regulate chromosome segregation. However, less is known about the function of Haspin kinase in regulatory networks in plant cells. Here, we show that inhibition of Haspin kinase with 5-iodotubercidin (5-ITu) in BY-2 cells delayed chromosome alignment. Haspin inhibition also prevented the centromeric localization of Aurora3 kinase (AUR3) kinase and disrupted its function. This suggested that Haspin kinase plays a role in the specific positioning of AUR3 on chromosomes in plant cells, a function conserved in animals. The results also indicated that Haspin and AUR3 kinases are involved in the same pathway, which regulates chromosome alignment during prometa-/metaphase. Remarkably, Haspin inhibition by 5-ITu also led to severe cytokinesis defect, resulting in binuclear cells with a partially formed cell plate. The 5-ITu treatment did not affect microtubules, AUR1/2, or the NACK-PQR pathway; however, it did alter the distribution of actin filaments on the cell plate. Together, these results suggested that Haspin has several functions in regulating cell division in plant cells: in the localization of AUR3 on centromeres, and in regulating late cell plate expansion during cytokinesis.

Keywords: Aurora3 kinase, BY-2, Chromosome alignment, Cytokinesis, Haspin kinase

Introduction

Mitosis is a complex process with strict regulation, the failure of which leads to serious diseases and disorders of growth and development (Kastan and Bartek 2004; Normand and King 2010). However, many of the regulatory elements studied in animals are unknown players in the field of plant mitosis. Moreover, plant cell division, while sharing the main stages of eukaryotic mitosis, is distinguished from animal mitosis by the formation of the preprophase band and cytokinesis (Cyr and Fisher 2012). The requirement for complex cellular machinery to build a new cell wall, together with the importance of timing and position, suggest that plants have evolved a unique regulatory network to maintain cytokinesis.

Phosphorylation plays a central role in regulating mitosis, for example, in mitotic checkpoints, spindle function, chromosome segregation, and cytokinesis (Nigg, 2001). Haspin (haploid germ cell-specific nuclear protein kinase) is a typical protein kinase that is conserved in many eukaryotic lineages including animals, fungi, and plants (Tanaka et al. 1999; Higgins 2001). In animal cells, Haspin phosphorylates histone H3 at Thr3, which promotes recruitment of the chromosome passenger complex (CPC) with Aurora B kinase as the enzymatic subunit (Wang et al. 2010; Kelly et al. 2010; Yamagishi et al. 2010). Haspin knockdown by RNAi was shown to prevent proper chromosome alignment at the metaphase plate (Dai et al. 2005; Higgins 2010), and chemical inhibition of Haspin prevented the centromeric localization of Aurora B, leading to impaired chromosome congression and spindle assembly checkpoint override (De Antoni et al. 2012; Wang et al. 2012). Activation of Haspin kinase early in mitosis is triggered by Cdk1-Polo kinase1 pathway (Zhou *et al.* 2014); further Aurora B-phosphorylation feedback loop amplifies the signal (Wang *et al.* 2011, Qian *et al.* 2013). The kinetochore kinase Bub1 pathway provides

the positional anchor that leads to accumulation of H3T3ph on centromeres by prometaphase (Wang et al. 2011).

However, according to recent studies on fungi and plants, Haspin may play additional roles in regulating cell division. In yeast, there is no evidence of H3T3ph, and therefore, the function of Haspin cannot be explained by the animal model. Nevertheless, a budding yeast Haspin knockout mutant showed transient mitotic arrest and severe abnormalities in spindle positioning and in the distribution of polarity cues (Panigada et al. 2013). In plants has been identified in *Arabidopsis thaliana* as AtHaspin (Kurihara et al. 2011; Ashtiyani et al. 2011). The AtHaspin kinase domain shows rather low similarity (38%) to human Haspin; however, the amino acid residues that bind ATP and Mg^{2+} are conserved. *In vitro* experiments have shown that AtHaspin phosphorylates histone H3 at Thr3 and, surprisingly, also at Thr11 (Kurihara et al. 2011). In a transgenic plant expressing AtHaspin-GFP driven by the native promoter, the GFP signal was observed during the embryo stage and in tissues with high cell-division activity, such as meristems. Moreover, a mutant overexpressing the kinase domain of AtHaspin showed delayed root growth and decreased size of the root meristem (Kurihara et al. 2011). Altered expression of AtHaspin kinase induced pleiotropic phenotypes with defects in floral organs and vascular tissue, study indicates that AtHaspin may also contribute to embryonic patterning (Ashtiyani et al. 2011).

Although the role of Haspin in regulating plant cell division remains unclear, other histone H3 kinases, the Aurora kinases, are known to function in plant cell division. Three members of the Aurora kinase family (AtAUR1, 2, and 3) have been identified in *A. thaliana*. In the *in vitro* experiments, all three AtAURs phosphorylated histone H3 at S10, and AtAUR3 also

phosphorylated histone H3 at S28 (Demidov et al. 2005; Kawabe et al. 2005; Kurihara et al. 2006). AtAUR3 kinase shows centromeric localization from prophase to metaphase. Inhibition of AtAUR3 led to a delay in chromosome alignment and aberrant chromosome segregation (Kurihara et al. 2006; Kurihara et al. 2008; Eswaran et al. 2009). Nevertheless, the relation between Haspin kinase and the Aurora family in plant cells has not been established yet. AtAUR1 and AtAUR2 are localized on the mitotic spindles during mitosis and on the cell plate during cytokinesis. AtAUR1 and AtAUR2 most likely have redundant functions in orientation of the cell division plane during plant development (Van Damme et al. 2011). Interestingly, research on yeasts has demonstrated that Haspin kinase is important for actin and polarity cues distribution during cytokinesis (Panigada et al. 2013). This implies that Haspin has role in regulating cytokinesis in different organisms.

Cytokinesis is distinctive feature in plant cell division due to the presence of the cell wall. Unlike the cell division mediated by the contractile ring animals and yeasts, plant cell division is achieved by phragmoplast-guided cell plate formation and expansion towards the cell periphery (Jürgens 2005). The phragmoplast consists mainly of microtubule (MT) and actin filaments that form a highly dynamic structure, and changes in this structure are essential for cytokinesis (Lee and Liu 2013; McMichael and Bednarek 2013). Although the significance of the phragmoplast in plant cell division is explicit, the factors involved in its regulation not fully understood yet. One pathway that is known to play a role in regulation is the NACK-PQR cascade, which governs cytokinesis via regulating phragmoplast MTs (Nishihama et al. 2002; Nishihama et al. 2001; Sasabe and Machida 2012). The NACK-PQR cascade is downregulated by CDKs until metaphase; then, from anaphase, the interaction between mitotic kinesin NACK1 and MAPK

kinase kinase NPK1 activates the cascade (Sasabe et al. 2011). All of the components of the cascade concentrate at the midzone of the phragmoplast during cytokinesis (Sasabe and Machida 2012). The downstream MAPKs phosphorylate microtubule-associated protein 65 (MAP65), which in turn promotes MT turnover and cell plate expansion (Sasabe et al. 2006).

Although actin filaments are a prominent part of the phragmoplast array, the role of actin remains highly controversial. Disruption of actin with various drugs, such as profilin (Valster et al. 1997), bistheonellide A (Hoshino et al. 2003; Higaki et al. 2008), or Latrunculin B (Kojo et al. 2013) caused delayed cell plate expansion and other aberrations in cytokinesis. In addition, some studies have shown a link between actin function and the motor protein, myosin (Molchan et al. 2002). Myosin VIII together with actin was shown to guide phragmoplast expansion to the cortical division site in moss and tobacco (Wu and Bezanilla 2014). Thus, although actin filaments appear to be essential for proper cytokinesis in plant cells, their exact role and interactions remain unclear. Although there is no evidence that Haspin kinase affects cytokinesis in animal cells, Haspin kinase was shown to be important for regulating cell division in a budding yeast (Panigada et al. 2013).

5-Iodotubercidin (5-ITu) is a small molecule that inhibits Haspin kinase activity in mammalian cells, which in turn, displaces CPC with Aurora B from centromeres (De Antoni et al. 2012; Wang et al. 2012). Here, using 5-ITu, we examined the function of Haspin kinase in regulating cell division in tobacco BY-2 cells. We show that inhibition of plant Haspin kinase led to a delay in chromosome alignment during prometa-/metaphase. Moreover, 5-ITu treatment affected AUR3 localization and function on centromeres. We also report that inhibition of Haspin kinase with 5-ITu treatment led to severe cytokinesis defect, resulting in incomplete cell plate

formation and two nuclei inside one cell. These data provide evidence that Haspin kinase has a dual role in regulating cell division in plant cells.

Results

5-ITu is a valid inhibitor of the plant Haspin kinase

5-ITu potently targets the ATP-binding site of human Haspin kinase (Eswaran et al. 2009). The selectivity of inhibitors for Haspin kinase has been investigated thoughtfully via *in vitro* assays and temperature-shift assays in several studies (Balzano et al. 2011; Fedorov et al. 2012; De Antoni et al. 2012). Experimental analyses showed that 5-ITu only weakly inhibited, or did not inhibit, the majority of mitotic kinases including Cdk1–Cyclin B, Aurora A, Aurora B–INCENP, Nek2, Bub1, Plk1, and Mps1. To verify that 5-ITu is a valid inhibitor for plant Haspin kinase, we conducted both *in vitro* and *in vivo* assays. The *in vitro* kinase assay was performed using purified GST-AtHaspin and GST-AtHaspin-KD (kinase-dead) with or without inhibitors. We screened a broad range of 5-ITu concentrations in this experiment. Phosphorylation of the GST-histoneH3 tail at specific residues was checked by immunoblotting using specific antibodies. As shown in our previous study (Kurihara et al. 2011), GST-AtHaspin phosphorylated H3 at Thr3 and Thr11, while GST-AtHaspin-KD showed no kinase activity. 5-ITu inhibited H3T3ph in a concentration-dependent manner, but it did not affect H3T11ph (Fig. 1A). To confirm the specificity of 5-ITu against Haspin kinase, the same *in vitro* kinase assay was performed with purified GST-AtAUR3, which phosphorylates histone H3 at Ser10 and Ser28 (Kurihara et al. 2006). GST-AtAUR3 phosphorylated histone H3 at Ser10, and this H3S10ph was inhibited by hesperadin, an Aurora kinase inhibitor (Kurihara et al. 2006), at a final concentration of 10 μ M. However, 5-ITu did not inhibit H3S10 phosphorylation by GST-AtAUR3, suggesting that 5-ITu acts as a specific plant Haspin kinase inhibitor, as for Haspin in mammalian cells.

To evaluate the effect of 5-ITu on Haspin *in vivo*, we used *Nicotiana tabacum* L. cv. Bright Yellow 2 (tobacco BY-2) cultured cells. BY-2 cells have high cell division activity and large chromosomes, making them suitable for research on plant cell division. We added 5-ITu at various concentrations to the BY-2 cell culture, and then incubated the cells for a further 24 h. After fixing cells, we performed indirect immunofluorescence analyses using an anti-H3T3ph antibody. The signals of H3T3ph were decreased between 0.1 and 0.5 μM 5-ITu. At 1 μM , H3T3ph could not be detected visually (Fig. 1B). Quantitative data (Fig. 1C) represents concentration-dependent reduction in the H3T3ph signal normalized against the DAPI signal. *In vivo* assay H3T3ph was more sensitive to inhibition, reaching maximum at 1 μM 5-ITu. Given that *in vivo* studies better reflect kinase behavior in living cells, we considered the concentration of 1 μM 5-ITu sufficient to inhibit Haspin activity in BY-2 cells.

To analyze the gene encoding Haspin kinase in BY-2 cells, we obtained a candidate Haspin kinase sequence from the cDNA library of BY-2 cells created by RNA-Seq. We cloned the candidate Haspin cDNA from the cDNA library of 3-day-old BY-2 cells using specific primers designed based on the RNA-Seq data. The identified cDNA, designated as *NtHaspin* (*N. tabacum* Haspin-related gene; accession no. LC052296), was 1,902-bp long and encoded a protein of 633 amino acid residues. The amino acid sequence of NtHaspin showed 68% and 39% similarities with AtHaspin and human Haspin in the kinase domain, respectively. Similar to AtHaspin, NtHaspin contained the conserved residues that act as ATP- and Mg^{2+} ion-binding sites and are important for histone H3 phosphorylation in the catalytic cleft (Kurihara et al. 2011). To observe the subcellular localization of NtHaspin throughout the cell cycle, we made a transgenic BY-2 line expressing NtHaspin-mClover and tdTomato-CenH3 (a marker for the

centromeric region of chromosomes). During interphase, NtHaspin was located in the cytoplasm (Fig. 1D). After nuclear envelope breakdown (NEBD), it invaded the nuclear region. During prometaphase and metaphase, NtHaspin was widely distributed over the mitotic spindle, and a stronger signal was observed on chromosomes aligned at the equatorial plate. During cytokinesis, starting from late telophase, NtHaspin was localized between two newly formed nuclei at the phragmoplast area. Following phragmoplast expansion, NtHaspin moved towards the cell periphery. This localization pattern of NtHaspin was similar to that of AtHaspin (Kurihara et al. 2011). 5-ITu treatment did not affect NtHaspin localization (Fig. 1D), suggesting that the kinase activity of NtHaspin is not required for its localization.

Localization of NtAUR3 on centromeres is associated with NtHaspin function

We conducted another *in vivo* assay to check H3T3ph and H3T11ph throughout the cell cycle, using anti-H3S28ph antibodies as a negative control for immunostaining (Fig. 2). BY-2 cells treated with DMSO had strong signals from both H3T3ph and H3T11ph during prometaphase and metaphase, and H3S28ph was observed on centromeres from prophase until anaphase. As expected, treatment with 1 μ M 5-ITu strongly decreased H3T3ph, and, surprisingly, H3T11ph and H3S28ph as well. However, the phosphorylation at H3S10 by AtAUR3 kinase was not affected by 5-ITu *in vitro*, even at higher concentrations of 5-ITu (Fig. 1A). The same result was reported previously for mammalian cells (Balzano et al. 2011).

To determine whether the localization of AUR3 was affected by 5-ITu treatment, we performed indirect immunofluorescence analyses using anti-H3T3ph and anti-H3S28ph antibodies in BY-2 cells expressing NtAUR3 (accession no. LC052299)-mClover. In order to

enhance signal from NtAUR3-mClover, anti-GFP antibody were used for immunostaining as well. Compared with control cells incubated with DMSO, those incubated with 5-ITu showed weak or no NtAUR3-mClover signals in the centromeric region and no H3S28 phosphorylation activity (Fig. 3). To rule out the possibility that direct inhibition of NtAUR3-mClover caused kinase mislocalization, we tested the Aurora kinase inhibitor hesperadin at a final concentration of 5 μ M. Unlike the effect of 5-ITu, the cells treated with hesperadin retained the NtAUR3-mClover signal on centromeres, although H3S28 phosphorylation was inhibited (Fig. 3). Live-cell imaging of BY-2 cells expressing NtAUR3-mClover confirmed that 5-ITu displaced NtAUR3-mClover from the centromeres (see Supplementary Movie S1, S2). These results suggested that under 5-ITu treatment, the decreased H3S28ph signal was because of NtAUR3 displacement from centromeres, rather than direct inhibition of the kinase function of NtAUR3. Furthermore, we presume that NtAUR3 localization in the centromeric region of chromosomes during mitosis is associated with NtHaspin kinase function.

5-ITu treatment increases duration of mitosis and alters chromosome alignment

As shown in Fig. 4, 5-ITu treatment affected cell division in BY-2 cells. To analyze cell growth and cell cycle progression, we calculated the mitotic index after a 24-h incubation with 5-ITu at a broad range of concentrations. BY-2 cells showed a concentration-dependent decrease in the mitotic index. The minimum mitotic index was $0.92\% \pm 0.28\%$ ($n = 4$ experiments) at 1 μ M 5-ITu (Fig. 4A). This result indicated that 5-ITu can prevent BY-2 cells from entering mitosis. Hence, 5-ITu slowed the growth rate of the cell culture. Quantitative data obtained from live-cell imaging showed that mitosis took longer under inhibitor treatment (Fig.

4B). In control cells treated with DMSO, the average length of mitosis, from pro- till telophase, was 60 ± 3 min ($n = 67$). However, average mitosis length grew up to 113 ± 7 min ($n = 13$) in BY-2 cells incubated with $1 \mu\text{M}$ 5-ITu.

Live-cell imaging in BY-2 cells expressing tdTomato-CenH3 revealed that under 5-ITu treatment, the prolonged duration of mitosis was because of a delay in chromosome alignment during prometa/metaphase (Fig. 4C, lagging chromosomes indicated with white arrowheads). However, the spindle assembly checkpoint was not disturbed, thus metaphase/anaphase transition occurred no sooner than all chromosomes were aligned at the equatorial plate (Supplementary Movie S3). Together, these results showed that BY-2 cells in which Haspin kinase was inhibited by 5-ITu remained in the prometaphase/metaphase stages for longer, which increased the duration of mitosis.

Inhibition of Haspin kinase causes cytokinesis defect in BY-2 cells

In the live-cell imaging experiments (Fig. 1D), we frequently observed bizarre cytokinesis in cells treated with 5-ITu. This prompted us to investigate the effect of 5-ITu on the final stage of cell division. For this purpose, we made a transgenic BY-2 line expressing GFP-KNOLLE (syntaxin KNOLLE is a specific cell plate marker; Lauber et al. 1997) to observe the cytokinesis process. As expected, control cells treated with DMSO showed normal cytokinesis, in which cell plate formation progressed centrifugally until the plate fused with the lateral cell walls (Fig. 5A). However, BY-2 cells treated with 5-ITu showed cytokinesis defect (Fig. 5A). The initiation of the cell plate also started at late telophase, and the cell plate expanded and usually fused with one lateral cell wall. At this point, the process stopped and the cell plate did

not continue expansion to the other side of the cell. Even after 2 h, there was no progress in cytokinesis and the cells still had a half-formed cell plate. Another characteristic of the cytokinesis defect was the blocked movement of nuclei, which remained attached to the half-formed cell plate (Fig. 5A). We also checked accumulation of callose during cytokinesis by aniline blue staining (Supplementary Fig. S1). Both control (DMSO) and 5-ITu treated cells show bright blue fluorescence in the cell plate. It indicates that vesicle traffic to the cell plate is not affected, which is also supported by normal distribution of KNOLLE.

Other members of the Aurora family, AtAUR1 and AtAUR2, were previously described as kinases important for cytokinesis in plants (Van Damme et al. 2011). We checked the localization of NtAUR1 (accession no. LC052297)-mClover and NtAUR2 (accession no. LC052298)-mClover in BY-2 cells throughout the cell cycle under 5-ITu treatment. In control cells treated with DMSO, both NtAUR1 and NtAUR2 were concentrated on the nuclear membrane prior to NEBD and on the mitotic spindle during mitosis. Later, they were localized in the phragmoplast region (Fig. 5B; Supplementary Fig. S2). These localization patterns were consistent with those of AtAUR1 and AtAUR2 (Demidov et al. 2005; Kawabe et al. 2005). Treatment with 5-ITu did not affect the distribution of NtAUR1 and NtAUR2 during cell division (Fig. 5B; Supplementary Fig. S2). These results suggested that Haspin kinase activity is not required for the functions of NtAUR1/2 in cytokinesis.

The NACK-PQR pathway, a NACK1 kinesin-like protein and mitogen activated protein kinase (MAPK) cascade, is a key regulator of plant cytokinesis. This pathway regulates the assembly of phragmoplast MTs (Nishihama et al. 2001; Nishihama et al. 2002; Soyano et al. 2003). There are several members involved in the cascade, however, up to current knowledge

the most downstream is NtMAP65-1, which phosphorylation stimulates phragmoplast expansion in tobacco (Sasabe et al. 2006). To determine the effect of 5-ITu on the NACK-PQR pathway, we performed indirect immunofluorescence staining using anti-NtMAP65-1, anti-NtMAP65-1ph, and anti- α -tubulin antibodies (Fig. 5C). In control cells, both MAP65-1 and MAP65-1ph were co-localized with MTs in the phragmoplast. 5-ITu treatment did not affect the localization or the phosphorylation of MAP65-1 (Fig. 5C). These data suggested that NtHaspin kinase inhibition with 5-ITu did not affect the NACK-PQR pathway.

5-ITu disturbs actin dynamics during cytokinesis

Actin filaments are also involved in cytokinesis. Expansion of the cell plate is guided by MT and actin filaments array, which dynamic changes are essential for proper cytokinesis (Lee and Liu 2013). A Haspin kinase knockout mutant of yeast showed altered actin distribution during mitosis (Panigada et al. 2013). To explore the role of the cytoskeleton in the cytokinesis defects caused by 5-ITu, we tested the effect of 5-ITu on BY-2 cells expressing three markers: GFP- α -tubulin (microtubules), tdTomato-CenH3 (centromeres), and Lifeact-mTurquoise2 (F-actin) (Fig. 6A). In control cells treated with DMSO, MTs formed the mitotic spindle, and both MTs and actin filaments were concentrated around the cell plate at the start of cytokinesis. As the cell plate expanded, cytoskeleton elements depolymerized in the center and repolymerized along the edge of the growing cell plate (Fig. 6A). In the cells treated with 5-ITu, the MT distribution was the same as that in the control, but there was lower concentration of actin filaments at the cell plate.

Next, we explored whether changes in actin dynamics alone could explain the cytokinesis defect. BY-2 cells expressing GFP-KNOLLE were treated with 2 μ M Latrunculin B, a drug that disrupts the actin cytoskeleton (Wakatsuki et al. 2001). Disruption of actin filaments led to a significant delay in cytokinesis (Fig. 6B). Corresponding with the results published by other groups (Kojo et al. 2013), cell plate expansion was aberrant and tilted cell planes were frequently observed. However, the late cell plate expansion was not completely blocked by Latrunculin B, as opposed to the arrested cell plate expansion caused by 5-ITu treatment. Previous studies of drugs other than Latrunculin B have not been able to demonstrate that the absence of actin filaments alone leads to severe cytokinesis defects (Nishimura et al. 2003). Quantitative data of cell plate expansion rates is presented in Supplementary Fig. S3. Comparing to Latrunculin B, 5-ITu treatment has stronger effect of the cell plate expansion. Average cell plate size is also smallest in 5-ITu sample, which reflects cytokinesis defect and complete inhibition of the cell plate expansion, which occurred in some cells. Taken together, these results indicate that other factors beside actin are involved in the cytokinesis defect caused by 5-ITu.

DISCUSSION

Based on the results of this study, we have expanded the hypothesis about the role of Haspin kinase in regulating cell division in plants (Fig. 7). Our experiments with the chemical inhibitor 5-ITu revealed that Haspin kinase is likely to contribute to chromosome alignment during prometaphase/metaphase, and affects late cell plate expansion during cytokinesis.

We showed that 5-ITu inhibits H3T3ph both *in vitro* and *in vivo*; however, H3T11ph was inhibited by 5-ITu only *in vivo*. We observed that 1 μ M 5-ITu was sufficient to inhibit Haspin kinase function in BY-2 cells, compared with 10 μ M used in experiments on mammalian cells (De Antoni et al. 2012; Wang et al. 2012). Based on these results, we conclude that 5-ITu is an effective inhibitor of the plant Haspin kinase. Several studies have analyzed 5-ITu selectivity in mammalian cells (Balzano et al. 2011; De Antoni et al. 2012); however, corresponding experiments have not been conducted for plant kinases so far. Here, we tested the specificity of 5-ITu for the AUR3 kinase, as the most likely candidate for the Haspin regulatory pathway. In plant cells, AUR3 kinase has two known substrates, H3S10 and H3S28; both are phosphorylated in the pericentromeric region of chromosomes from prophase until metaphase (Kawabe et al. 2005). In the *in vitro* assay, 5-ITu did not inhibit H3S10ph even at high concentrations, although the AUR-specific inhibitor hesperadin significantly reduced the phosphorylation level (Fig. 1A). However, in the *in vivo* assay, BY-2 cells treated with 5-ITu showed no detectable H3S28ph, consistent with the displacement of NtAUR3 from the centromeric region. Hesperadin treatment reduced H3S28ph, yet it did not affect NtAUR3 localization. These data showed that under 5-ITu treatment, NtAUR3 mislocalization affects its function at the pericentromeric region of chromosomes. This result is consistent with studies on mammalian cells, where inhibition of

human Haspin displaced Aurora B kinase from centromeres, and interfered with the phosphorylation activity of Aurora B on the inner kinetochores, but not with other Aurora B functions (De Antoni et al. 2012; Wang et al. 2012). Although Aurora kinase family is diversified in plants and animals, Aurora B kinase from mammalian cells and AUR3 kinase from plant cells share localization areas during mitosis and at least some functions, including centromeric phosphorylation of H3S10 and H3S28. It indicates that relationship between Aurora kinase family and Haspin kinase is be conserved. Nevertheless, it should be noted that histone H3 phosphorylation patterns differ between in mammalian and plant cells. In animal cells, H3T3 is phosphorylated on centromeres during prometaphase and metaphase (Dai et al. 2005; Markaki et al. 2009), but in plants, the H3T3ph signal is evenly distributed on chromosomes (Kurihara et al. 2011). We presume that Haspin kinase function is essential for the centromeric localization of AUR3 in plant cells, but whether it is associated with H3T3ph or depends upon other interactions is open for further investigation.

The cell division of BY-2 cells treated with 5-ITu showed several deviations from normal cell division. Mitosis took significantly longer because of a delay in chromosome alignment along the equatorial plane in prometa/metaphase. Previously, Haspin downregulation by RNAi was shown to cause chromosome misalignment and partial loss of chromatid cohesion (Dai et al. 2006; Dai et al. 2009). Treatment with 5-ITu had a similar effect in HeLa cells (De Antoni et al. 2012; Wang et al. 2012). However, in BY-2 cells, 5-ITu did not cause spindle assembly checkpoint override or defects during anaphase, possibly because of the lower concentrations of 5-ITu used in our experiments. Direct inhibition of AUR3 with hesperadin was shown to cause a delay in chromosome alignment in plant cells (Kurihara et al. 2008), indicating that the

centromeric function of AUR3 is important for prometa/metaphase progression. These findings suggest that Haspin and Aurora are involved in the same pathway, where Haspin is upstream and provides spatial information, recruiting AUR3 to centromeres. Therefore, 5-ITu inhibition of Haspin function also downregulates AUR3, leading to the delay in chromosome alignment.

Here, we also report previously uncharacterized cytokinesis defect in BY-2 cells treated with 5-ITu (Fig. 5A). In BY-2 cells treated with 5-ITu, late cell plate expansion was completely inhibited, and the movement of nuclei was blocked. Up to our knowledge, in animal cells, cytokinesis abnormalities have not been reported for 5-ITu treatment or Haspin downregulation by RNAi. Therefore, we presume that 5-ITu affects process or regulatory pathway unique for plant cell division. Analysis of cell culture ploidy revealed that 5-ITu treatment increases percentage of 4C cells in BY-2 cells (Supplementary Fig. S4). We suggest that 5-ITu-induced increase in ploidy reflects two process in cell culture. 5-ITu decreases the mitotic index, however it is possible that cells duplicate DNA, but do not enter mitosis for some reason. Live-imaging showed that during cell division chromosomes separate normally and two nuclei are formed. However, nuclei do not separate and stay attached to the cell plate. Such nuclei also can contribute to increased 4C signal.

We checked several elements involved in cytokinesis in plant cells: distribution of KNOLLE, accumulation of callose, AUR1 and AUR2, the NACK-PQR pathway, and MT and actin dynamics. Based on KNOLLE distribution and normal accumulation of callose, we suggest that 5-ITu does not inhibit vesicle transport to the cell plate. Therefore cytokinesis defect is caused by other reasons. Localization of NtAUR1 and NtAUR2 was not affected by 5-ITu treatment. The roles of the AUR1/2 pathway and its targets during cytokinesis are currently unknown; however,

the involvement of AUR1/2 in the 5-ITu phenotype did not seem likely. The *Arabidopsis* double mutant *aur1aur2* showed defective cell division orientation throughout development, but cell plate expansion was unaffected (Van Damme et al. 2011). Moreover, there is no evidence that Haspin interacts with other members of the Aurora family aside from Aurora B (or AUR3 in plants). The NACK-PQR pathway, which regulates MT turnover and phragmoplast expansion, was also unaffected by 5-ITu treatment. Although we have not tested all of the components of the NACK-PQR pathway in this study, the phosphorylation and localization of the most downstream member, MT-associated protein NtMAP65-1, remained intact under 5-ITu treatment. Surprisingly, 5-ITu treatment had no visual impact on MT dynamics, even though severe cytokinesis defects are usually associated with disturbed MT dynamics (Lee and Liu 2013). Thus, we consider that NtHaspin has no relationship with these pathways.

The phragmoplast consists of both MT and actin filaments, yet the role of actin in cytokinesis remains ambiguous. Here, we demonstrated that one characteristic of the 5-ITu-induced cytokinesis defect was impaired actin colocalization to the cell plate (Fig. 6A). The reasons for the disrupted actin dynamics remain unclear; however, studies on yeast have demonstrated a link between Haspin kinase and actin distribution; that is, the Haspin kinase knockout mutant showed abnormal actin distribution during cytokinesis, which resulted in binuclear cells (Panigada et al. 2013). Furthermore, Haspin was shown to localize specifically in the region enriched with actin in mouse oocytes (Nguyen et al. 2014). Taken together, these observations and results suggest that the relationship between Haspin and actin is conserved in various species. Recently, the actomyosin-mechanism of phragmoplast guidance was reported in moss (Wu and Bezanilla 2014). Myosin VIII was shown to accumulate at MT plus ends and at

the cortical division zone, while F-actin connected the phragmoplast edge to the periphery membrane. It was suggested that Myosin VIII uses actin bridges to connect the phragmoplast MT to the cortical division site (Wu and Bezanilla 2014). Additionally, a phenotype very similar to that under 5-ITu treatment was observed in *Tradescantia* stamen hair cells treated with an inhibitor of the myosin light-chain kinase. These cells showed inefficient cytokinesis, up to complete inhibition late cell plate expansion (Molchan et al. 2002).

In summary, treatment of BY-2 cells with a Haspin kinase inhibitor led to severe cytokinesis defect, potentially caused by disturbed actomyosin-guided phragmoplast expansion. We suggest that the actomyosin complex and the distribution of polarity factors, such as formins, should be analyzed in further studies to establish their relationships with Haspin kinase.

Based on our data, we propose the following hypothesis for Haspin function in regulating cell division in plant cells (Fig. 7): during prometa/metaphase, Haspin kinase function is necessary for the centromeric localization of AUR3. One possibility is that H3T3ph is a conserved mechanism for recruitment of AUR3 to centromeres. As cell division progresses, Haspin appears to be involved in different pathways regulating late cell plate expansion. Inhibition of Haspin led to cytokinesis defect and the formation of binuclear cells. Other factors involved into this pathway are unknown (Fig. 7, Factor X); however, we suggest actomyosin as a prospective downstream candidate in the Haspin cascade.

Methods

Tobacco BY-2 cell culture

The tobacco BY-2 (*Nicotiana tabacum* L. cv. Bright Yellow 2) cell culture was maintained as described by Nagata et al. (1992). BY-2 cells were cultured in modified Linsmaier and Skoog medium on a rotary shaker at 100 r.p.m. at 26°C in the dark.

Cloning and transformation

For RNA-Seq analysis, BY-2 cells were cultured for 2, 5, and 7 days after transferring to fresh medium. Total RNA was extracted from the three cultures with a High Pure RNA Tissue Kit (Roche). A 1- μ g aliquot of the extracted RNA was converted to a cDNA library using a TruSeq RNA Library Prep Kit (Illumina). Single-end 59-bp reads were generated from the cDNA library by Genome analyzer Iix. Nearly 50 million short reads were obtained for each library, and a total 141 million short reads were assembled by Trinity software (Grabherr et al. 2011). We used BLAST search to find sequences for Haspin and Aurora kinase candidates using this assembled sequence as the database (Zhang et al. 2000). For further vector construction, mRNAs were isolated from 3-day-old BY-2 cells using Dynabeads Oligo (dT)₂₅ (Invitrogen) and cDNAs were synthesized by SuperScript III reverse transcriptase (Invitrogen). The PCR primers used in this study are listed in Supplementary Table S1. The cDNAs of *NtHaspin*, *NtAUR1*, *NtAUR2*, and *NtAUR3* were subcloned into the spUC-mClover vector, which contains the CaMV 35S promoter as described by Kurihara et al. (2011). The resulting 35Spro::cDNA-mClover was inserted into the binary vector pPZP211 (Hajdukiewicz et al. 1994). The Lifeact-mTurquoise2 sequence, which was obtained from Addgene (No. 36201), was also inserted into the pPZP211 vector. To

generate the GFP-KNOLLE marker, genomic DNA of *A. thaliana* (Columbia accession) was used as the template for PCR to amplify the genomic fragment containing the upstream (2.1 kb) and entire coding regions of *KNOLLE* (At1g08560). This fragment was cloned into the pENTR/D-TOPO vector (Invitrogen), and subjected to an In-Fusion cloning reaction (In-Fusion HD Cloning Kit, Takara Bio) to insert the EGFP fragment at the N terminus of *KNOLLE*. The resulting GFP-KNOLLE fusion construct was then subcloned using LR clonase enzyme mix (Invitrogen) into the Gateway-compatible binary vector pZP211-GW, which contains the Gateway cassette (Gateway Vector Conversion System, Invitrogen) at the *Sma*I site of pZP211. The binary vectors were introduced into *Agrobacterium tumefaciens* strain EHA105. Transformation of BY-2 cells and BY-GTRC (expressing GFP- α -tubulin-RFP-CenH3) cells (Kurihara et al. 2008) was performed as described elsewhere (Kurihara et al. 2011).

In vitro kinase assay

The *in vitro* kinase assay was performed with purified GST-AtHaspin or GST-AtHaspin-KD or GST-AtAUR3 and GST-histone H3 tail as the substrate, as described previously (Kurihara et al. 2006; Kurihara et al. 2011). In brief, inhibitor (5-ITu or hesperadin) was added to the reaction mixture at the desired concentration before adding ATP. Phosphorylated histone H3 was determined by immunoblotting using 1:1000 dilutions of rabbit polyclonal antibodies against H3T3ph and H3T11ph (Upstate Biotechnology) and rabbit polyclonal antibodies against H3S10ph (Millipore). Immunoreactive proteins on the PVDF membranes were detected with a 1:10000 dilution of peroxidase-conjugated goat anti-rabbit IgG antibody (KPL) and Immobilon

Western Chemiluminescent HRP Substrate (Millipore) using a luminescent image analyzer (LAS-4000 mini; GE Healthcare).

Fluorescence microscopy

We essentially followed the inhibitor treatment and immunostaining procedures described previously (Kurihara et al. 2006). For the inhibitor treatment, 2-day-old BY-2 cells were incubated with the desired concentration of inhibitor 24 h before fixation. Cells were fixed using 4% (w/v) PFA in PBS and placed on coverslips pre-treated with poly-L-lysine. Cell walls were briefly digested with an enzyme mixture consisting of 2% (w/v) cellulose and 0.5% (w/v) pectolyase in PBS. Next, the cells were permeabilized using 0.5% Triton X-100 in PBS, then blocked with 4% (w/v) BSA in PBS and incubated with appropriate primary antibodies diluted in PBS overnight at 4°C. We used a 1:500 dilution of rabbit polyclonal antibodies to H3T3ph and H3T11ph (Upstate Biotechnology), a 1:500 dilution of rat monoclonal antibodies to H3S28ph (Abcam), a 1:500 dilution of goat polyclonal antibodies to GFP (Abcam), a 1:200 dilution of mouse monoclonal antibodies to α -tubulin (Sigma), and 1:100 dilutions of rabbit polyclonal antibodies to NtMAP65-1 α (anti-MAP65) and Thr-579- phosphorylated NtMAP65-1 α (anti-pT579MAP65) (Sasabe et al. 2006). After the primary antibody reaction, cells were washed twice in PBS and then incubated with the respective secondary antibodies at the following dilutions in PBS for 3 h at room temperature: 1:200 dilutions of Alexa 594-conjugated goat anti-rabbit IgG antibodies, Alexa 488-conjugated goat anti-rat IgG antibodies, and Alexa 488-conjugated goat anti-mouse antibody (Invitrogen Molecular Probes). Cells were washed twice in PBS, and then mounted with

DAPI solution (2 $\mu\text{g}/\text{ml}$). Images were acquired with an Olympus BX-51 fluorescence microscope.

For aniline blue staining, we followed protocol described by Nishihama et al. (2001) with the following modifications: cells were fixed with 0.1% glutaraldehyde in 50 mM sodium phosphate buffer (pH 7.5) for 1 h, washed three times in 50 mM Na_2HPO_4 . Cells were stained with 0.1% aniline blue in 50 mM Na_2HPO_4 .

Flow Cytometry

Wild-type, 3-day-old BY-2 culture was treated with 1 μM 5-ITu, 5 μM Hesperadin or DMSO (control). After 24 hr cells were collected and frozen in liquid N_2 . Frozen pellets were used for nuclei extraction using CyStain UV Precise P kit (Partec, Germany) following manufacture's instructions. DNA content was analyzed using Sony SH800 cell sorter.

Live-cell imaging

BY-2 cells expressing NtHaspin-mClover or GFP-KNOLLE were observed using a confocal microscope (CV1000; Yokogawa Electric). BY-2 cells expressing NtAUR1,2,3-mClover or BY-2 cells expressing GFP- α -tubulin, CenH3-tdTomato, and Lifeact-mTurquoise2 were observed using a fluorescence microscope (IX-83; Olympus) equipped with a Nipkow disk confocal unit (CSU-W1; Yokogawa Electric). For inhibitor treatments, cells were incubated with the desired concentration of inhibitor for 1 h before observation. Images were processed using ImageJ software (<http://rsbweb.nih.gov/ij/index.html>) and Adobe Photoshop CS6 (Adobe Systems, Inc.).

References

Ashtiyani, R.K., Moghaddam, A.M., Schubert, V., Rutten, T., Fuchs, J., Demidov, D., et al. (2011)

AtHaspin phosphorylates histone H3 at threonine 3 during mitosis and contributes to embryonic patterning in Arabidopsis. *Plant J.* 68: 443-454.

Balzano, D., Santaguida, S., Musacchio, A. and Villa, F. (2011) A general framework for inhibitor resistance in protein kinases. *Chem. Biol.* 18: 966-975.

Cyr, R.J. and Fisher, D. (2012) Plant cell division and its unique features. *eLS.*

Dai, J., Sultan, S., Taylor, S.S. and Higgins, J.M. (2005) The kinase haspin is required for mitotic histone H3 Thr 3 phosphorylation and normal metaphase chromosome alignment. *Genes Dev.* 19: 472-488.

Dai, J., Sullivan, B.A. and Higgins, J.M. (2006) Regulation of mitotic chromosome cohesion by Haspin and Aurora B. *Dev. Cell* 11: 741-750.

Dai, J., Kateneva, A.V. and Higgins, J.M. (2009) Studies of haspin-depleted cells reveal that spindle-pole integrity in mitosis requires chromosome cohesion. *J. Cell Sci.* 122: 4168-4176.

De Antoni, A., Maffini, S., Knapp, S., Musacchio, A. and Santaguida, S. (2012) A small-molecule inhibitor of Haspin alters the kinetochore functions of Aurora B. *J. Cell Biol.* 199: 269-284.

Demidov, D., Van Damme, D., Geelen, D., Blattner, F.R. and Houben, A. (2005) Identification and dynamics of two classes of aurora-like kinases in *Arabidopsis* and other plants. *Plant Cell* 17: 836-848.

Eswaran, J., Patnaik, D., Filippakopoulos, P., Wang, F., Stein, R.L., Murray, J.W., et al. (2009) Structure and functional characterization of the atypical human kinase haspin. *Proc. Natl. Acad. Sci. U. S. A.* 106: 20198-20203.

Fedorov, O., Niesen, F.H. and Knapp, S. (2012) Kinase inhibitor selectivity profiling using differential scanning fluorimetry. *Methods Mol. Biol.* 795: 109-118.

Grabherr, M.G., Haas, B.J., Yassour, M., Levin, J.Z., Thompson, D.A., Amit, I., et al. (2011) Full-length transcriptome assembly from RNA-Seq data without a reference genome. *Nat. Biotechnol.* 29: 644-652.

Hajdukiewicz, P., Svab, Z. and Maliga, P. (1994) The small, versatile *pPZP* family of *Agrobacterium* binary vectors for plant transformation. *Plant Mol. Biol.* 25: 989-994.

Higaki, T., Kutsuna, N., Sano, T. and Hasezawa, S. (2008) Quantitative analysis of changes in actin microfilament contribution to cell plate development in plant cytokinesis. *BMC Plant Biol.* 8:

80.

Higgins, J.M. (2001) Haspin-like proteins: a new family of evolutionarily conserved putative eukaryotic protein kinases. *Protein Sci.* 10: 1677-1684.

Higgins, J.M. (2010) Haspin: a newly discovered regulator of mitotic chromosome behavior. *Chromosoma* 119: 137-147.

Hoshino, H., Yoneda, A., Kumagai, F. and Hasezawa, S. (2003) Roles of actin-depleted zone and preprophase band in determining the division site of higher-plant cells, a tobacco BY-2 cell line expressing GFP-tubulin. *Protoplasma* 222: 157-165.

Jürgens, G. (2005) Cytokinesis in higher plants. *Annu. Rev. Plant Biol.* 56: 281-299.

Kastan, M.B. and Bartek, J. (2004) Cell-cycle checkpoints and cancer. *Nature* 432: 316-323.

Kawabe, A., Matsunaga, S., Nakagawa, K., Kurihara, D., Yoneda, A., Hasezawa, S., et al. (2005) Characterization of plant Aurora kinases during mitosis. *Plant Mol. Biol.* 58: 1-13.

Kelly, A.E., Ghenoiu, C., Xue, J.Z., Zierhut, C., Kimura, H. and Funabiki, H. (2010) Survivin reads phosphorylated histone H3 threonine 3 to activate the mitotic kinase Aurora B. *Science* 330: 235-239.

Kojo, K.H., Higaki, T., Kutsuna, N., Yoshida, Y., Yasuhara, H. and Hasezawa, S. (2013) Roles of cortical actin microfilament patterning in division plane orientation in plants. *Plant Cell Physiol.* 54: 1491-1503.

Kurihara, D., Matsunaga, S., Kawabe, A., Fujimoto, S., Noda, M., Uchiyama, S., et al. (2006) Aurora kinase is required for chromosome segregation in tobacco BY-2 cells. *Plant J.* 48: 572-580.

Kurihara, D., Matsunaga, S., Uchiyama, S. and Fukui, K. (2008) Live cell imaging reveals plant aurora kinase has dual roles during mitosis. *Plant Cell Physiol.* 49: 1256-1261.

Kurihara, D., Matsunaga, S., Omura, T., Higashiyama, T. and Fukui, K. (2011) Identification and characterization of plant Haspin kinase as a histone H3 threonine kinase. *BMC Plant Biol.* 11: 73.

Lauber, M.H., Waizenegger, I., Steinmann, T., Schwarz, H., Mayer, U., Hwang, I., et al. (1997) The *Arabidopsis* KNOLLE protein is a cytokinesis-specific syntaxin. *J. Cell Biol.* 139: 1485-1493.

Lee, Y.R. and Liu, B. (2013) The rise and fall of the phragmoplast microtubule array. *Curr. Opin. Plant Biol.* 16: 757-763.

Markaki, Y., Christogianni, A., Politou, A.S. and Georgatos, S.D. (2009) Phosphorylation of histone H3 at Thr3 is part of a combinatorial pattern that marks and configures mitotic chromatin.

J. Cell Sci. 122: 2809-2819.

McMichael, C.M. and Bednarek, S.Y. (2013) Cytoskeletal and membrane dynamics during higher plant cytokinesis. *New Phytol.* 197: 1039-1057.

Molchan, T.M., Valster, A.H. and Hepler, P.K. (2002) Actomyosin promotes cell plate alignment and late lateral expansion in *Tradescantia* stamen hair cells. *Planta* 214: 683-693.

Nagata, T., Nemoto, Y. and Hasezawa, S. (1992) Tobacco BY-2 cell line as the "HeLa" cell in the cell biology of higher plants. *Int. Rev. Cytol.* 132: 1-30.

Nguyen, A.L., Gentilello, A.S., Balboula, A.Z., Shrivastava, V., Ohring, J. and Schindler, K. (2014) Phosphorylation of threonine 3 on histone H3 by haspin kinase is required for meiosis I in mouse oocytes. *J. Cell Sci.* 127: 5066-5078.

Nigg, E.A. (2001) Mitotic kinases as regulators of cell division and its checkpoints. *Nat. Rev. Mol. Cell Biol.* 2: 21-32.

Nishihama, R., Ishikawa, M., Araki, S., Soyano, T., Asada, T. and Machida, Y. (2001) The NPK1 mitogen-activated protein kinase kinase kinase is a regulator of cell-plate formation in plant cytokinesis. *Genes Dev.* 15: 352-363.

Nishihama, R., Soyano, T., Ishikawa, M., Araki, S., Tanaka, H., Asada, T., et al. (2002) Expansion of the cell plate in plant cytokinesis requires a kinesin-like protein/MAPKKK complex. *Cell* 109: 87-99.

Nishimura, T., Yokota, E., Wada, T., Shimmen, T. and Okada, K. (2003) An *Arabidopsis* *ACT2* dominant-negative mutation, which disturbs F-actin polymerization, reveals its distinctive function in root development. *Plant Cell Physiol.* 44: 1131-1140.

Normand, G. and King, R.W. (2010) Understanding cytokinesis failure. *Adv. Exp. Med. Biol.* 676: 27-55.

Panigada, D., Grianti, P., Nespoli, A., Rotondo, G., Castro, D.G., Quadri, R., et al. (2013) Yeast haspin kinase regulates polarity cues necessary for mitotic spindle positioning and is required to tolerate mitotic arrest. *Dev. Cell* 26: 483-495.

Qian, J., Beullens, M., Lesage, B. and Bollen, M. (2013) Aurora B defines its own chromosomal targeting by opposing the recruitment of the phosphatase scaffold Repo-Man. *Curr. Biol.* 23: 1136-1143.

Sasabe, M., Soyano, T., Takahashi, Y., Sonobe, S., Igarashi, H., Itoh, T.J., et al. (2006) Phosphorylation of NtMAP65-1 by a MAP kinase down-regulates its activity of microtubule bundling and stimulates progression of cytokinesis of tobacco cells. *Genes Dev.* 20: 1004-1014.

Sasabe, M., Boudolf, V., De Veylder, L., Inze, D., Genschik, P. and Machida, Y. (2011) Phosphorylation of a mitotic kinesin-like protein and a MAPKKK by cyclin-dependent kinases (CDKs) is involved in the transition to cytokinesis in plants. *Proc. Natl. Acad. Sci. U. S. A.* 108: 17844-17849.

Sasabe, M. and Machida, Y. (2012) Regulation of organization and function of microtubules by the mitogen-activated protein kinase cascade during plant cytokinesis. *Cytoskeleton (Hoboken)* 69: 913-918.

Soyano, T., Nishihama, R., Morikiyo, K., Ishikawa, M. and Machida, Y. (2003) NQK1/NtMEK1 is a MAPKK that acts in the NPK1 MAPKKK-mediated MAPK cascade and is required for plant cytokinesis. *Genes Dev.* 17: 1055-1067.

Tanaka, H., Yoshimura, Y., Nozaki, M., Yomogida, K., Tsuchida, J., Tosaka, Y., et al. (1999) Identification and characterization of a haploid germ cell-specific nuclear protein kinase (Haspin) in spermatid nuclei and its effects on somatic cells. *J. Biol. Chem.* 274: 17049-17057.

Valster, A.H., Pierson, E.S., Valenta, R., Hepler, P.K. and Emons, A. (1997) Probing the Plant Actin Cytoskeleton during Cytokinesis and Interphase by Profilin Microinjection. *Plant Cell* 9: 1815-1824.

Van Damme, D., De Rybel, B., Gudesblat, G., Demidov, D., Grunewald, W., De Smet, I., et al. (2011) *Arabidopsis* α Aurora kinases function in formative cell division plane orientation. *Plant Cell* 23: 4013-4024.

Wakatsuki, T., Schwab, B., Thompson, N.C. and Elson, E.L. (2001) Effects of cytochalasin D and latrunculin B on mechanical properties of cells. *J. Cell Sci.* 114: 1025-1036.

Wang, F., Dai, J., Daum, J.R., Niedzialkowska, E., Banerjee, B., Stukenberg, P.T., et al. (2010) Histone H3 Thr-3 phosphorylation by Haspin positions Aurora B at centromeres in mitosis. *Science* 330: 231-235.

Wang, F., Ulyanova, N.P., van der Waal, M.S., Patnaik, D., Lens, S.M. and Higgins, J.M. (2011) A positive feedback loop involving Haspin and Aurora B promotes CPC accumulation at centromeres in mitosis. *Curr. Biol.* 21: 1061-1069.

Wang, F., Ulyanova, N.P., Daum, J.R., Patnaik, D., Kateneva, A.V., Gorbisky, G.J., et al. (2012) Haspin inhibitors reveal centromeric functions of Aurora B in chromosome segregation. *J. Cell Biol.* 199: 251-268.

Wu, S.Z. and Bezanilla, M. (2014) Myosin VIII associates with microtubule ends and together with actin plays a role in guiding plant cell division. *Elife* 3.

Yamagishi, Y., Honda, T., Tanno, Y. and Watanabe, Y. (2010) Two histone marks establish the inner centromere and chromosome bi-orientation. *Science* 330: 239-243.

Zhang, Z., Schwartz, S., Wagner, L. and Miller, W. (2000) A greedy algorithm for aligning DNA sequences. *J. Comput. Biol.* 7: 203-214.

Zhou, L., Tian, X., Zhu, C., Wang, F. and Higgins, J.M. (2014) Polo-like kinase-1 triggers histone phosphorylation by Haspin in mitosis. *EMBO Rep.* 15: 273-281.

Funding

This work was supported by grants from the Japan Science and Technology Agency (ERATO project to T.H.).

Acknowledgments

We thank M. Sasabe for providing anti-MAP65 and anti pT579MAP65 antibodies, and Y. Nakano and S. Nasu for assistance in preparing materials. Microscopy was conducted at the Institute of Transformative Bio-Molecules (WPI-ITbM) of Nagoya University and supported by the Japan Advanced Plant Science Network.

Figure legends

Fig. 1. 5-ITu inhibits Haspin kinase function both *in vivo* and *in vitro*.

(A) *In vitro* kinase assay. GST-AtHaspin, GST-AtHaspin-KD, and GST-AtAUR3 were incubated with GST-H3 tail. Negative control: GST-H3 tail only. 5-ITu was added at a final concentration of 1, 5, 10 or 20 μM ; hesperadin was added at final concentration of 10 μM . Phosphorylated GST-H3 tail was immunostained using anti-H3T3ph, anti-H3T11ph, and anti-H3S28ph antibodies. (B) Phosphorylation of histone H3 at Thr3 *in vivo*. After 24-h incubation with indicated concentrations of 5-ITu, BY-2 cells were immunostained with anti-H3T3ph (red). DNA (blue) was stained with DAPI. Prometaphase stage is shown. Scale bar = 10 μm . (C) Quantitative data from experiment shown in B. Data was normalized to DAPI ratio. Values are mean \pm SD. Asterisks indicate significant differences compared with control (DMSO) (**** $p < 0.0001$; one-way ANOVA). (D) Localization of NtHaspin kinase in living BY-2 cells. Live-cell imaging was performed on BY-2 cells expressing NtHaspin-mClover (green in the merged plane) and tdTomato-CenH3 (red in the merged plane) after a 1-h treatment with DMSO (control) or 1 μM 5-ITu. Images are maximum projections of z-stack. Scale bar = 10 μm .

Fig. 2. Phosphorylation of histone H3 throughout the cell cycle *in vivo*.

After 24-h incubation with DMSO (control) or 1 μM 5-ITu, BY-2 cells were fixed and immunostained with the following antibody combinations: H3T3ph (red) + H3S28ph (green) or H3T11ph (red) + H3S28ph (green). DNA (blue) was stained with DAPI. Scale bar = 10 μm .

Fig. 3. NtAUR3 accumulation on centromeres associated with NtHaspin function.

BY-2 cells expressing NtAUR3-mClover were incubated with DMSO (control), 1 μ M 5-ITu, or 5 μ M hesperadin. After 24 h, cells were fixed and immunostained with antibody against H3T3ph (red) or H3S28ph (red). Anti-GFP antibody used to visualize NtAUR3-mClover (green), DNA (blue) was stained with DAPI. Prometaphase and metaphase are shown. Scale bar = 10 μ m.

Fig. 4. Effects of 5-ITu on BY-2 cell culture, mitosis duration, and chromosome alignment.

(A) BY-2 cells were treated with indicated concentrations of 5-ITu or DMSO (control) for 24 h. Mitotic index was calculated from $\geq 1,000$ cells in 4 independent experiments. Raw data is plotted on the graph. (B) Average duration of mitosis (from pro- till telophase) was calculated from live-imaging data. Live-cell imaging was performed on BY-2 cells after a 1-h treatment with DMSO (control) or indicated concentrations of 5-ITu. Graphs show mean value of ≥ 10 mitotic cells for each concentration \pm SD. Asterisks indicate significant differences compared with control (DMSO) (** $p < 0.01$, **** $p < 0.0001$; one-way ANOVA). (C) Chromosome alignment in living BY-2 cells. Imaging was performed on BY-2 cells expressing tdTomato-CenH3 after a 1-h treatment with DMSO (control) or 1 μ M 5-ITu. White arrows indicate lagging chromosomes under 5-ITu treatment. NEBD = nuclear envelope breakdown; Ana = anaphase. Images are maximum projections of z-stack acquired every 6 minute. Scale bar = 10 μ m.

Fig. 5. Cytokinesis defect in BY-2 cells under 5-ITu treatment.

(A) Restriction of syntaxin KNOLLE to cell plate. Live-cell imaging was performed on BY-2 cells expressing GFP-KNOLLE after a 1-h treatment with DMSO (control) or 1 μ M 5-ITu. Incomplete cell plate formation can be observed under inhibitor treatment. Nuclei are labeled with yellow

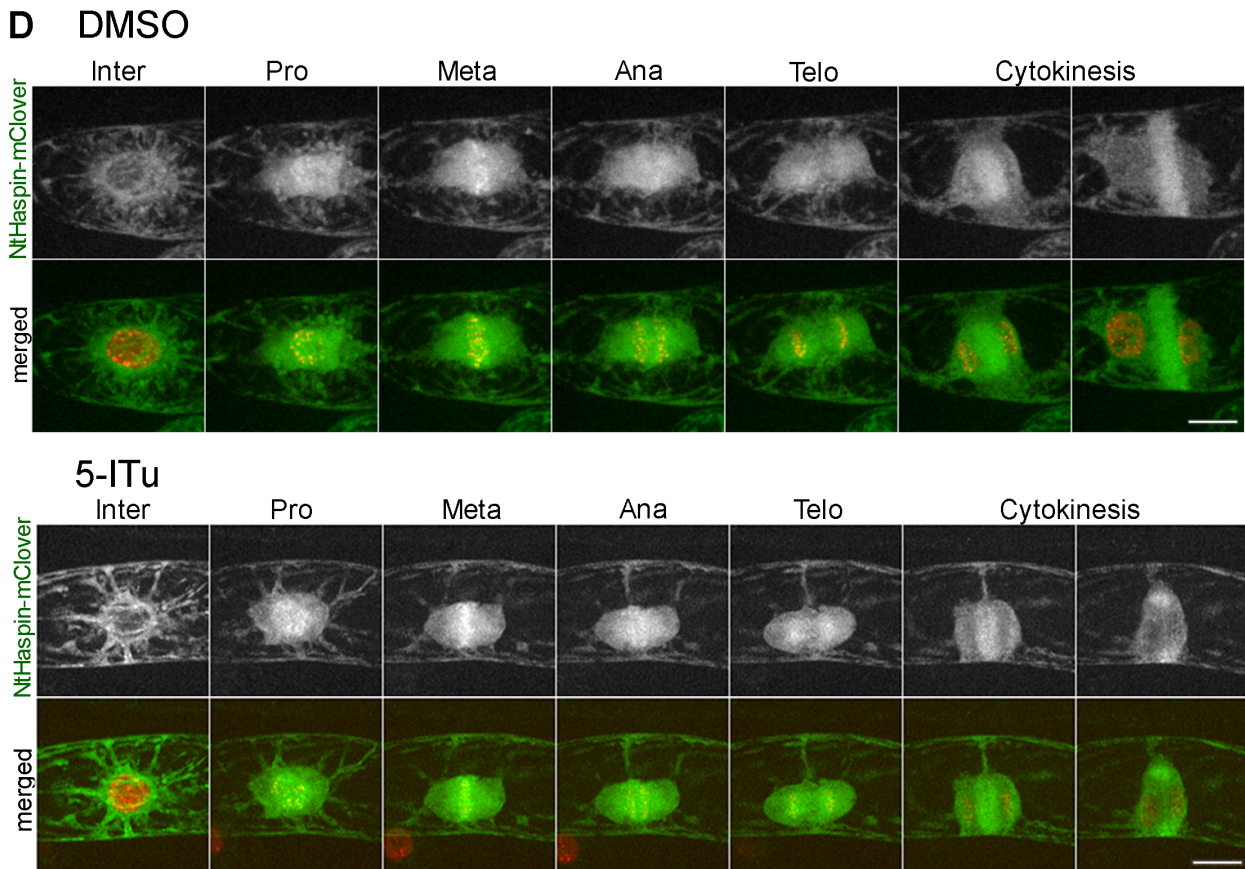
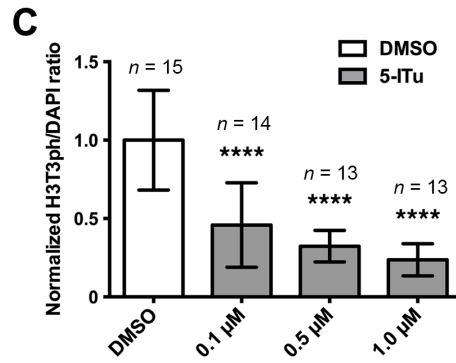
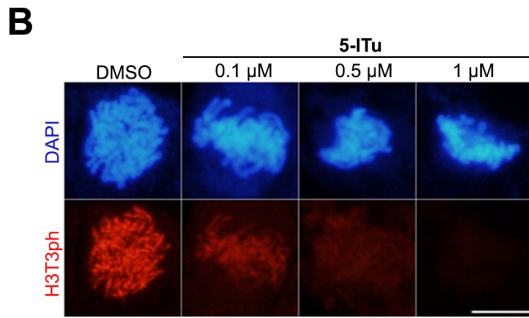
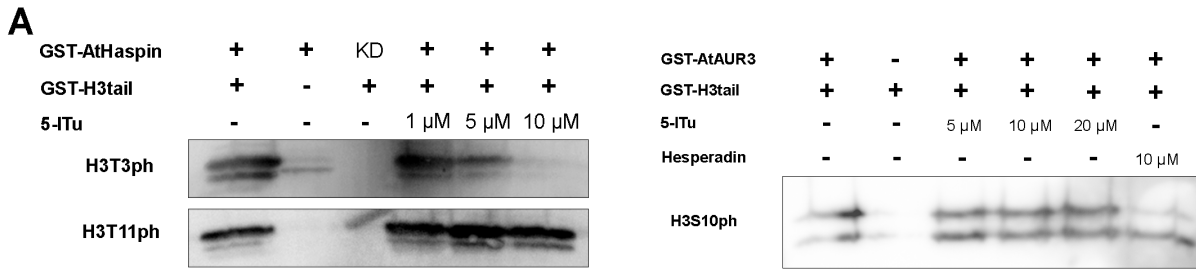
circles on merged plane. Images for GFP-KNOLLE and brightfield are a single focal plane. Numbers indicate time (hh: mm); a starting point of cytokinesis, when GFP-KNOLLE was first observed on the cell plate, is shown at 00:00 column. Inter = interphase, Pro = prophase, Meta = metaphase, Telo = telophase. Scale bar = 10 μ m. (B) Distribution of NtAUR1 throughout cell cycle. Live-cell imaging was performed on BY-2 cells expressing NtAUR1-mClover after a 1-h treatment with DMSO (control) or 1 μ M 5-ITu. Images are maximum projections of z-stack. Scale bar = 10 μ m. (C) Subcellular localization of NtMAP65-1 and NRK1-phosphorylated NtMAP65-1 during cytokinesis. BY-2 cells were treated with DMSO (control) or 1 μ M 5-ITu 24 h before fixation. Then, cells were stained with anti-MAP65-1 (red) or anti-MAP65-1ph (red) and anti- α -tubulin (green) antibodies. DNA (blue) was stained with DAPI. Scale bar = 10 μ m.

Fig. 6. Distribution of microtubules and actin filaments during mitosis and cytokinesis.

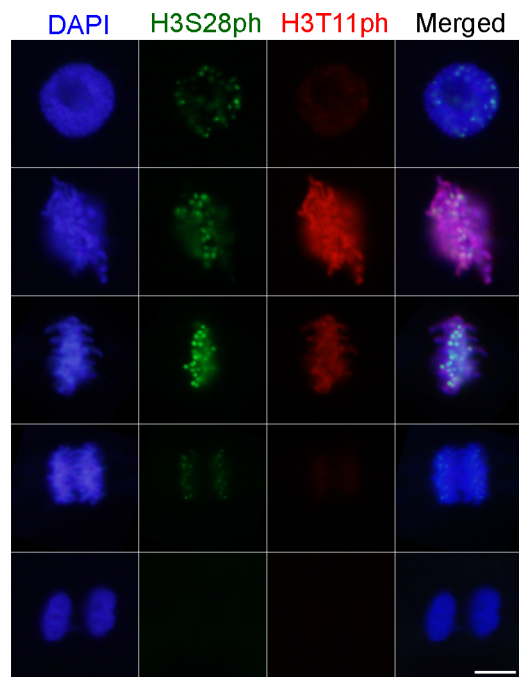
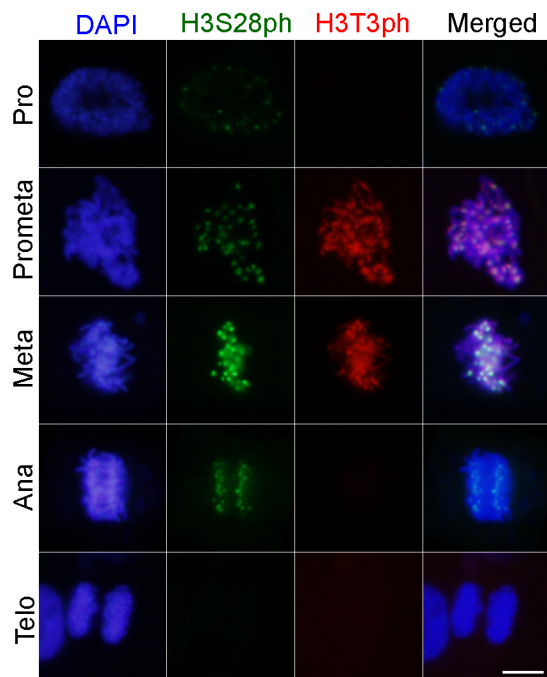
(A) Live-cell imaging was performed on BY-2 cells expressing GFP- α -tubulin (green), tdTomato-CenH3 (red), and Lifeact-mTurquoise2 (cyan) after a 1-h treatment with DMSO (control) or 1 μ M 5-ITu. Yellow arrows indicate concentration of actin at cell plate. Images are maximum projections of z-stack. Scale bar = 10 μ m. (B) Cytokinesis in BY-2 cells with disrupted actin filaments. Live-cell imaging was performed on BY-2 cells expressing GFP-KNOLLE after 3 h treatment with DMSO (control) or 2 μ M Latrunculin B. Images are a single focal plane acquired every 30 min. Scale bar = 10 μ m.

Fig. 7. Schematic representation of the role of Haspin in regulating plant cell division.

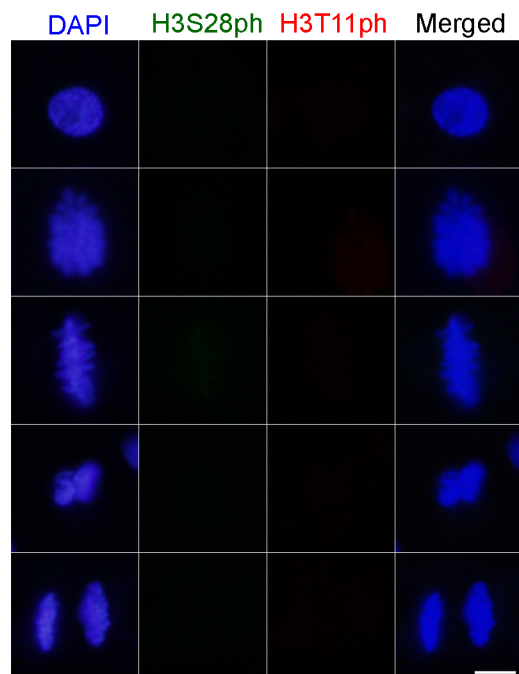
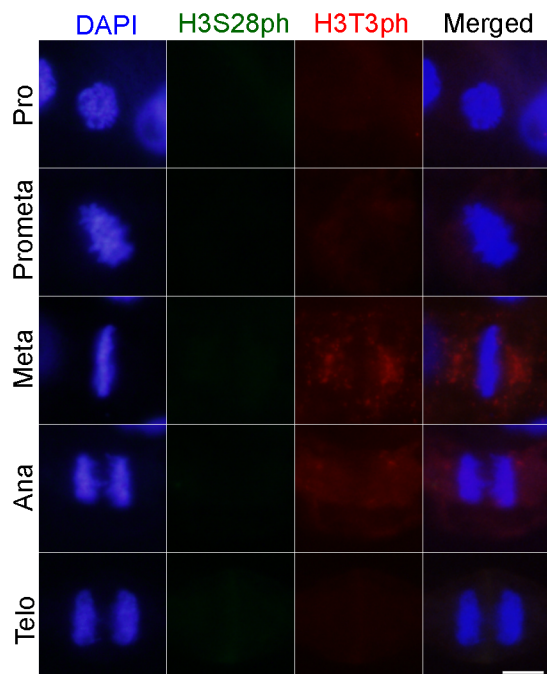
Inhibition of Haspin function by 5-ITu disturbs centromeric localization of AUR3. AUR3 mislocalization leads to delay in chromosome alignment during prometa-/metaphase. Later, inhibition of Haspin leads to cytokinesis failure due to arrest of late cell plate expansion; however, known regulatory pathways including AUR1/2 and NACK-PQR cascade are unaffected. Hypothetical Factor X, potentially the actomyosin complex, is proposed as the intermediate link in the Haspin cascade.

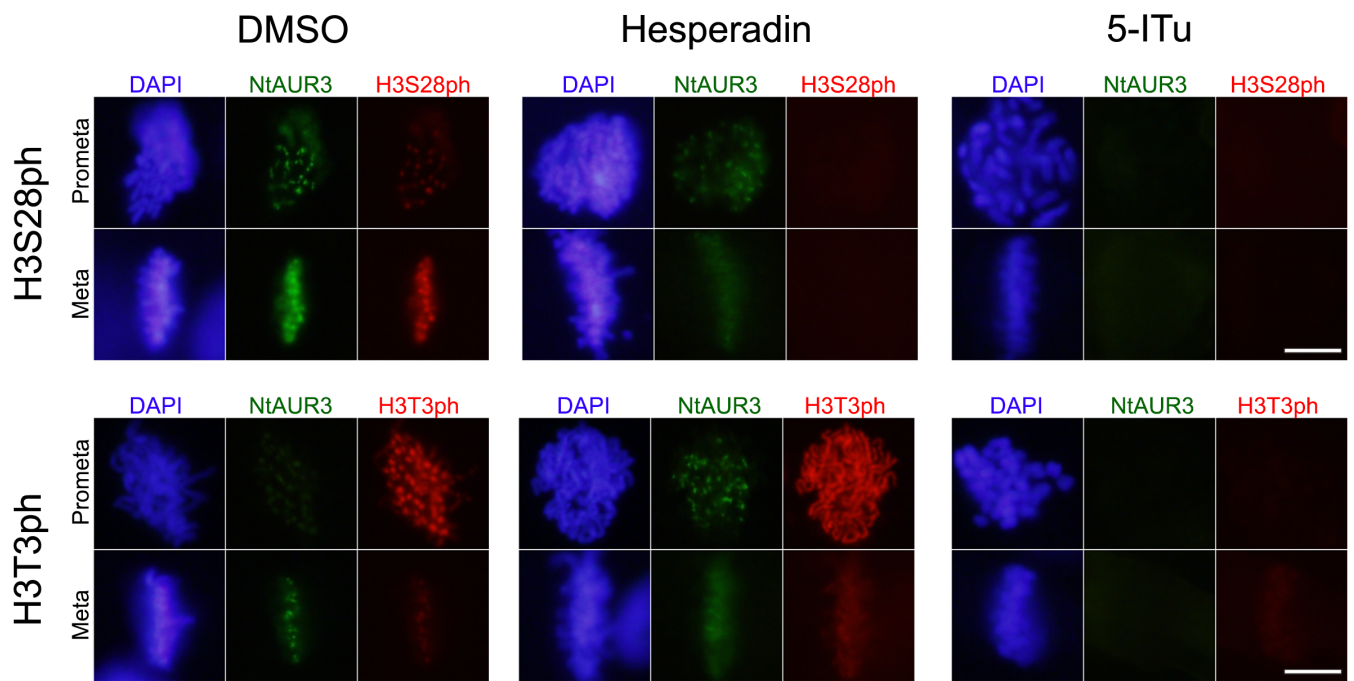


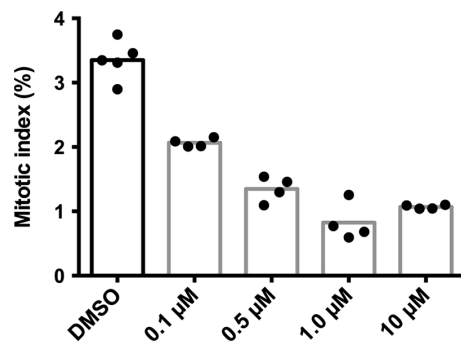
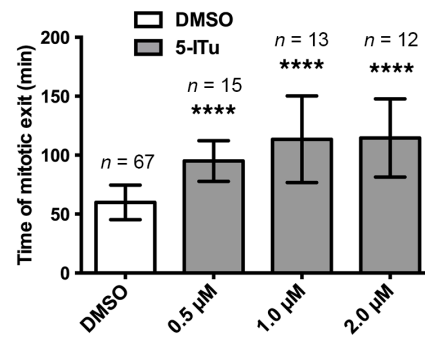
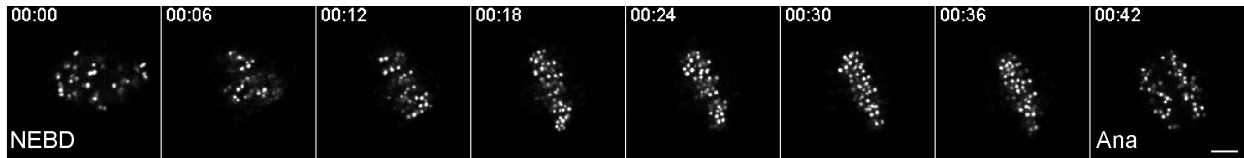
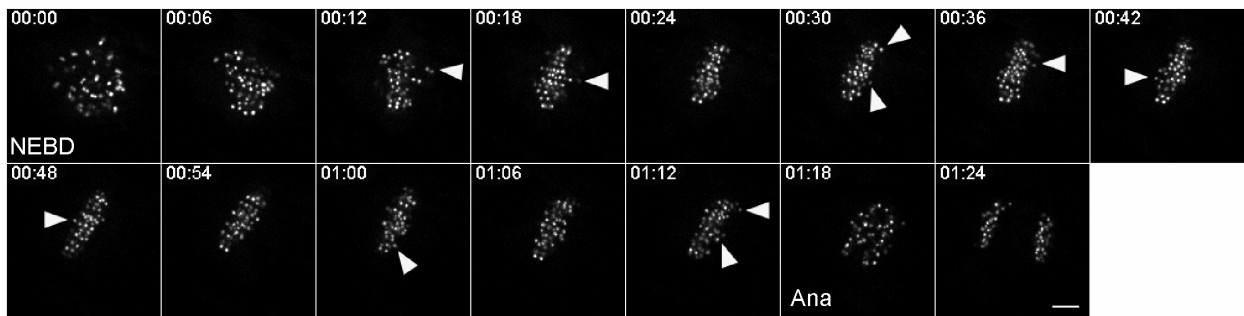
DMSO

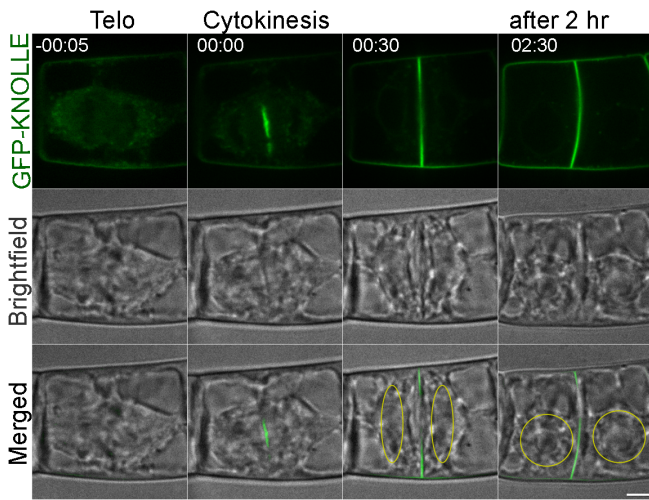
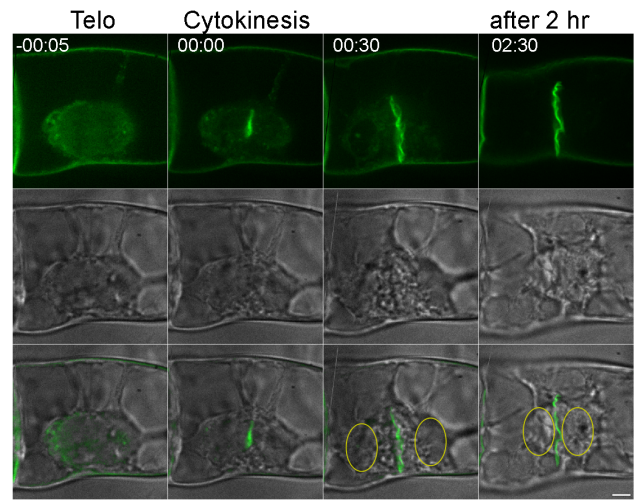
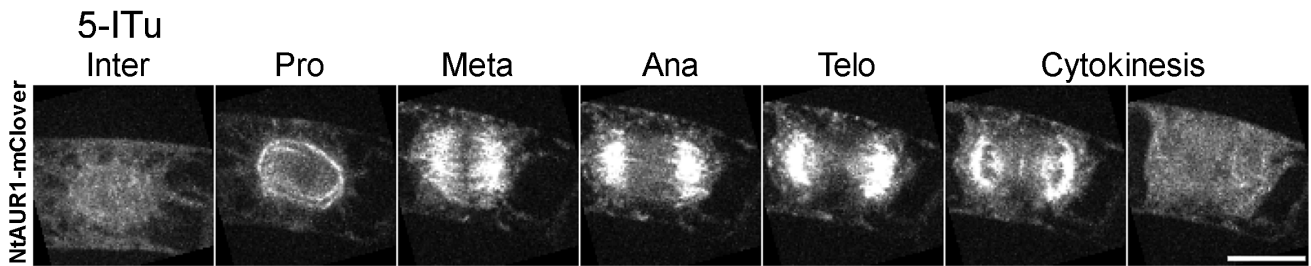
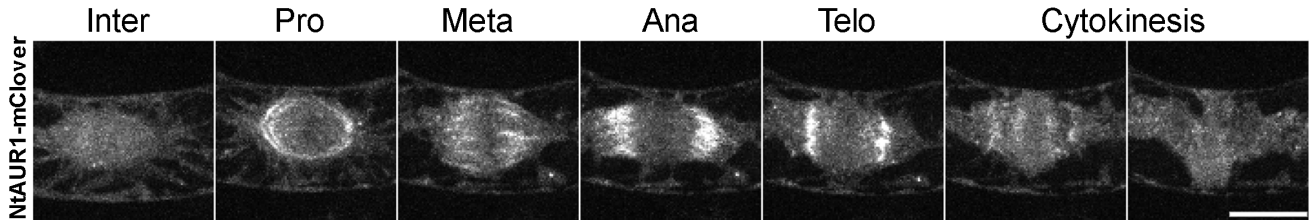
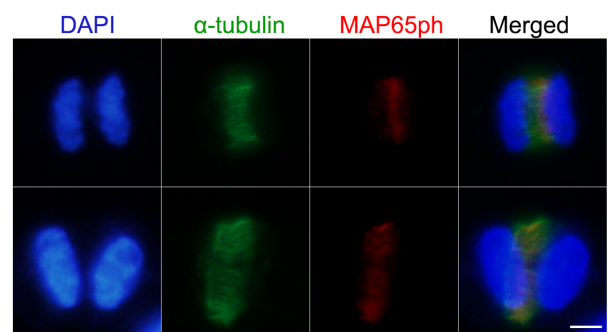
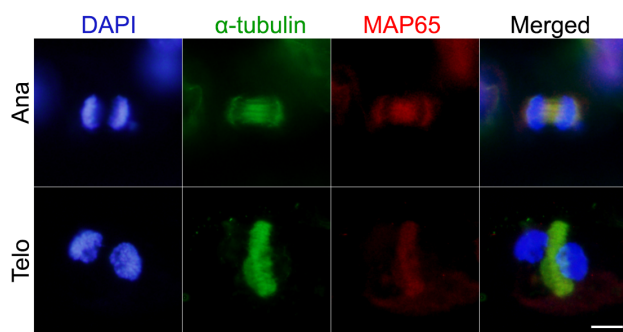
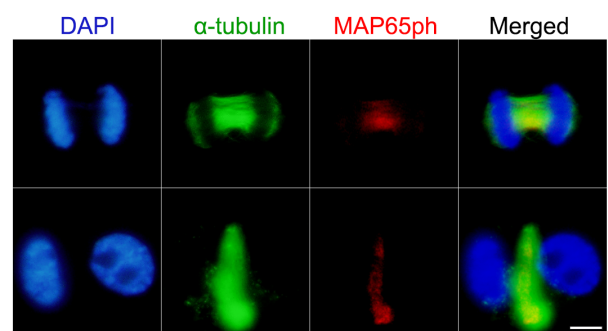
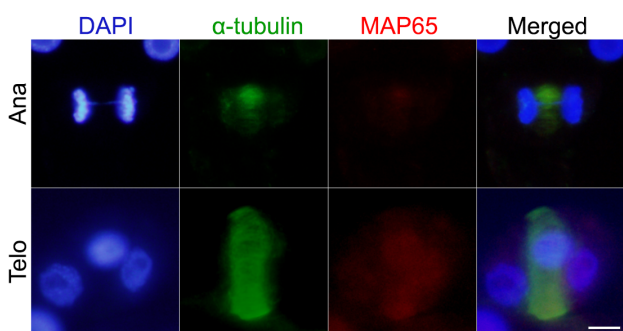


5-ITu

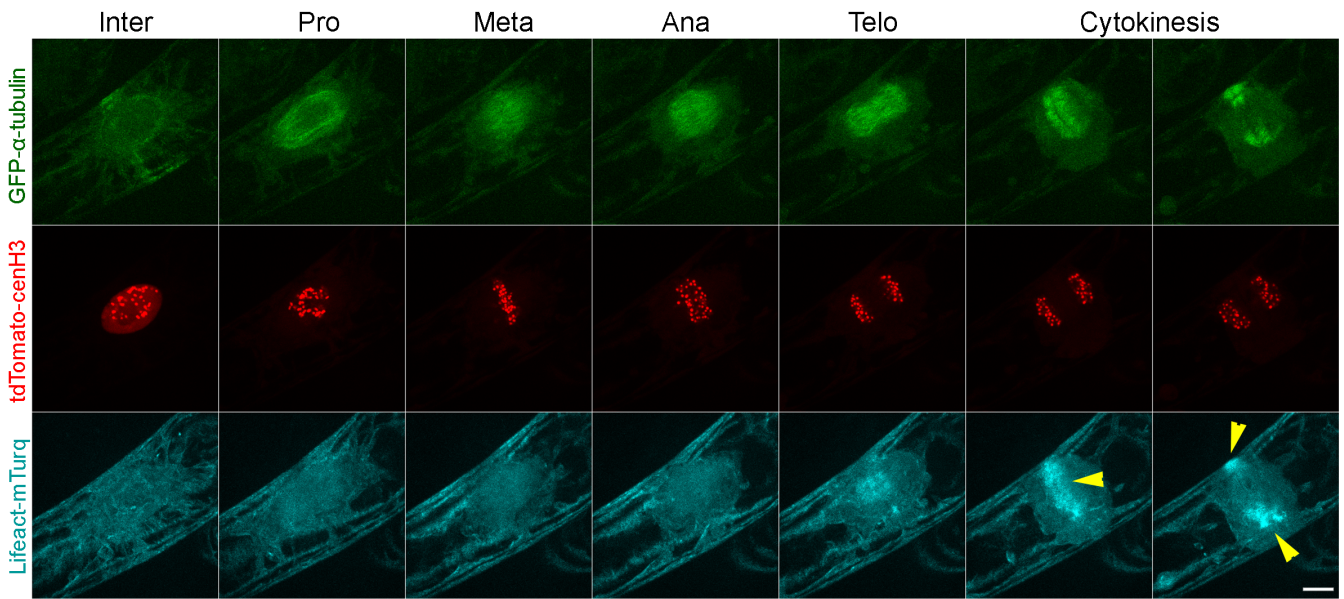




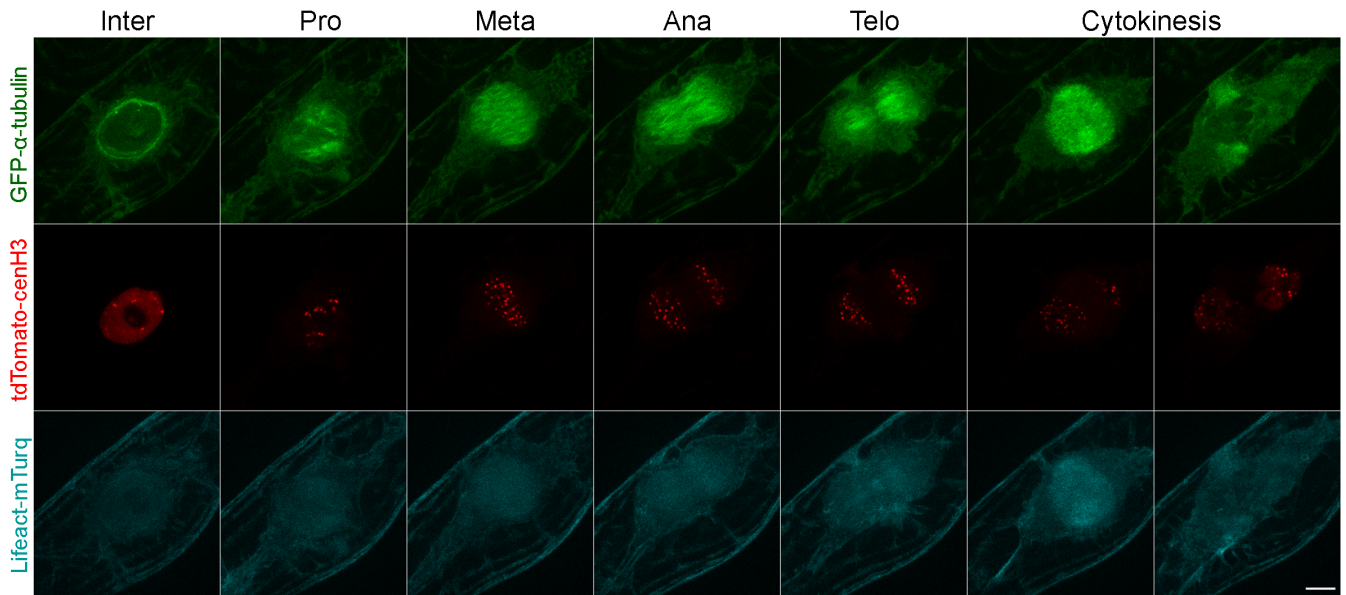
A**B****C DMSO****5-ITu**

A DMSO**5-ITu****B DMSO****C DMSO****5-ITu**

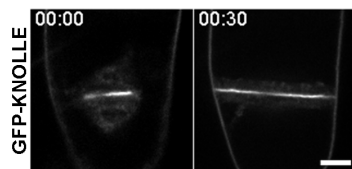
A DMSO



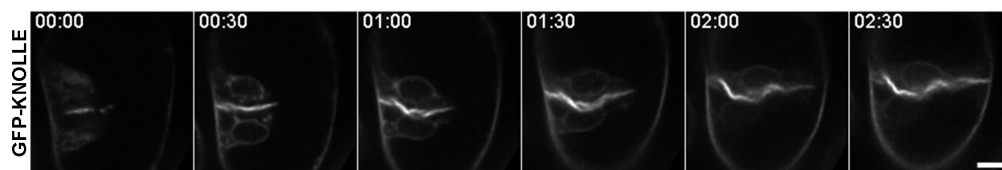
5-ITu

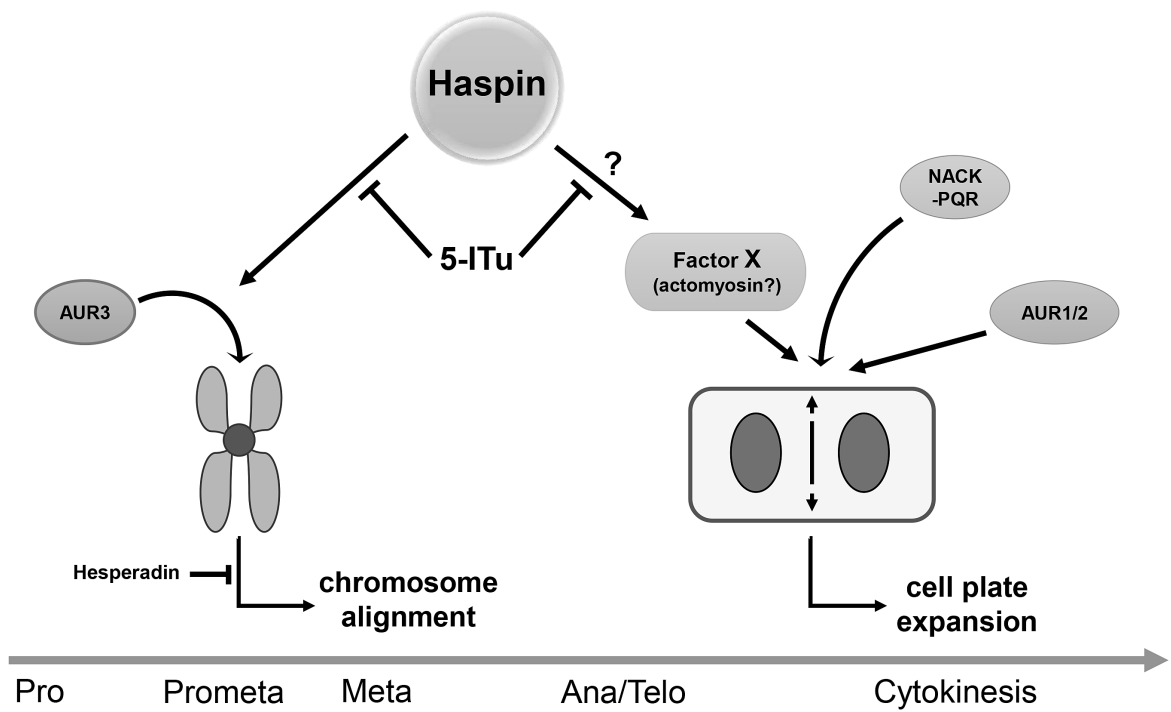


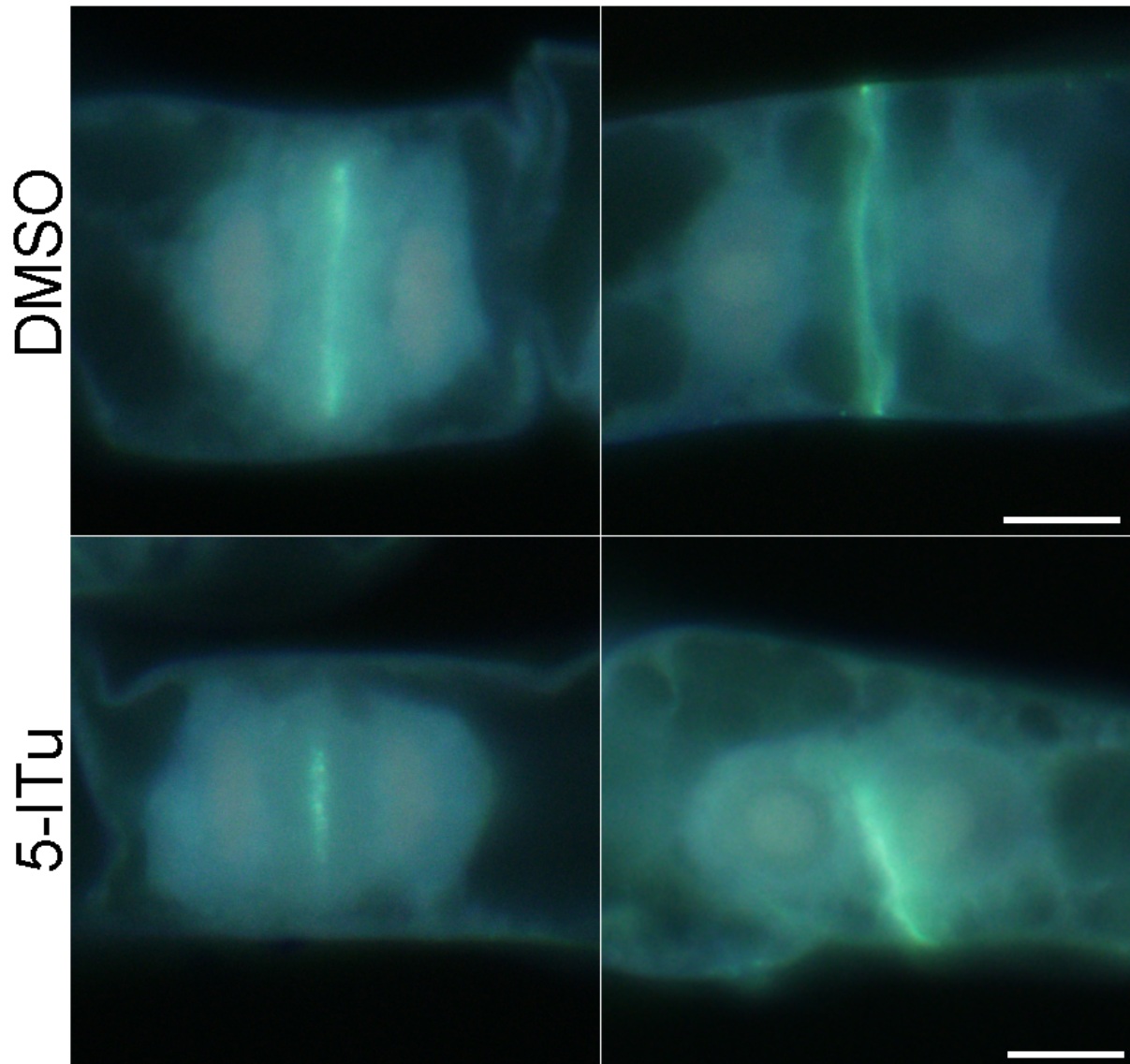
B DMSO



Latrunculin B



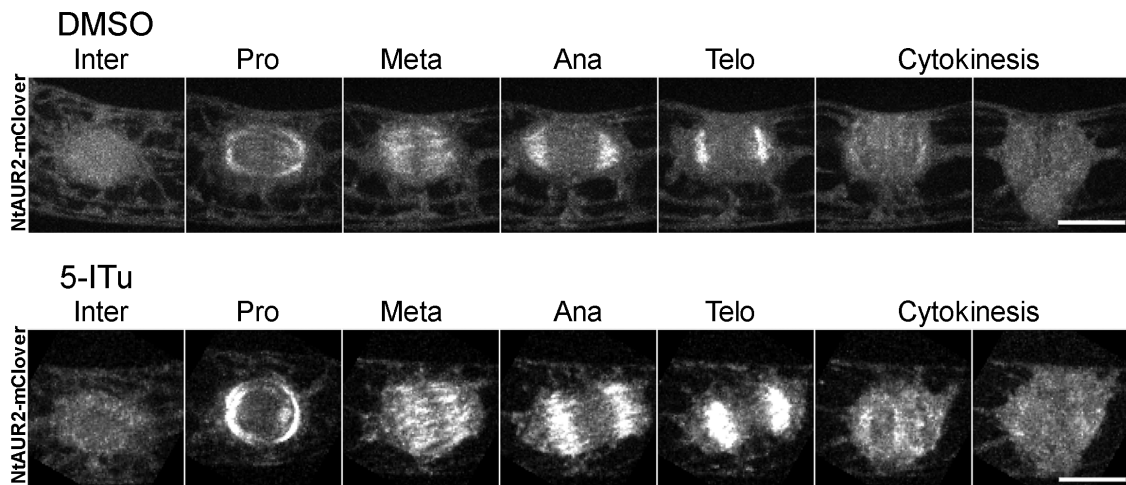




Supplementary Fig. S1. Accumulation of callose in the cell plate.

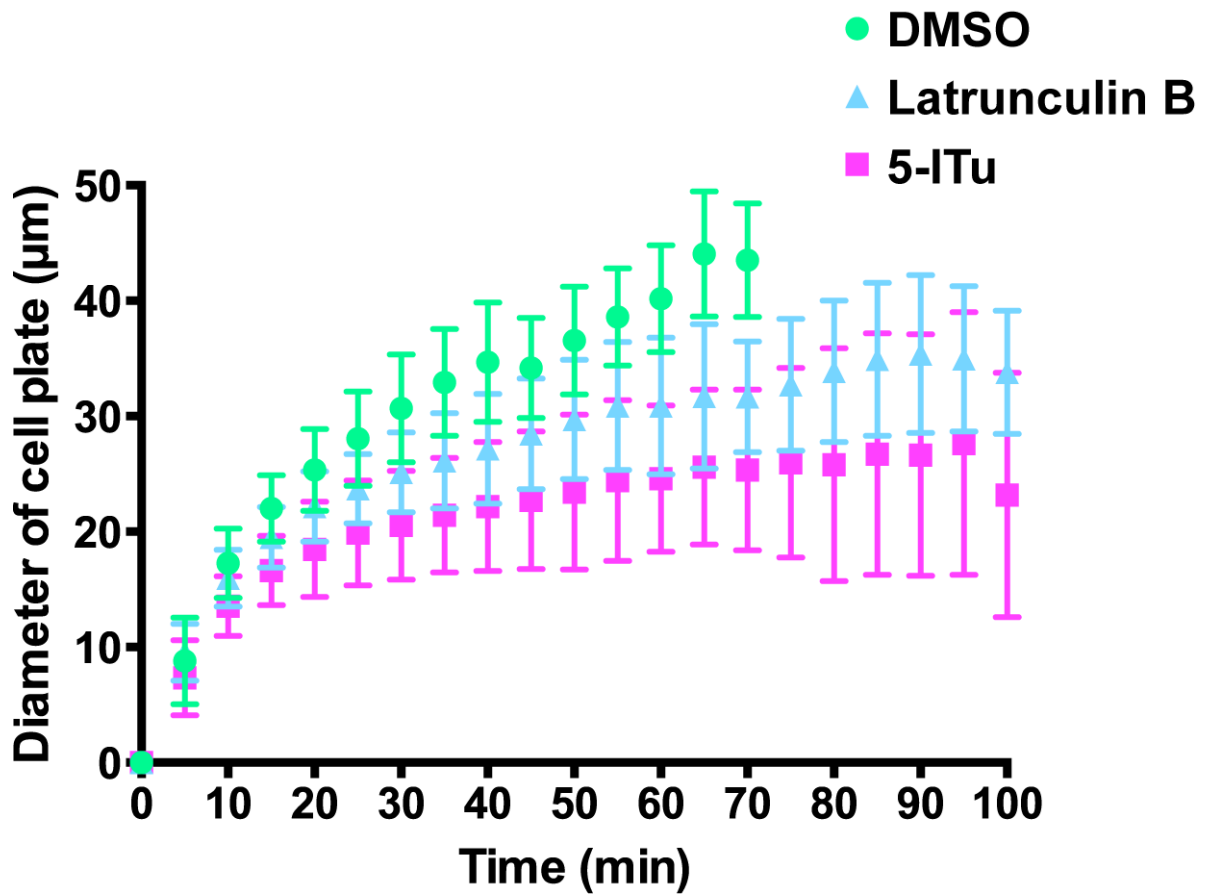
Aniline blue staining was performed in BY-2 cells after 24-h treatment with DMSO or 1 μ M 5-ITu.

Callose in the cell plate has yellow-blue fluorescence. Scale bar = 10 μ m.



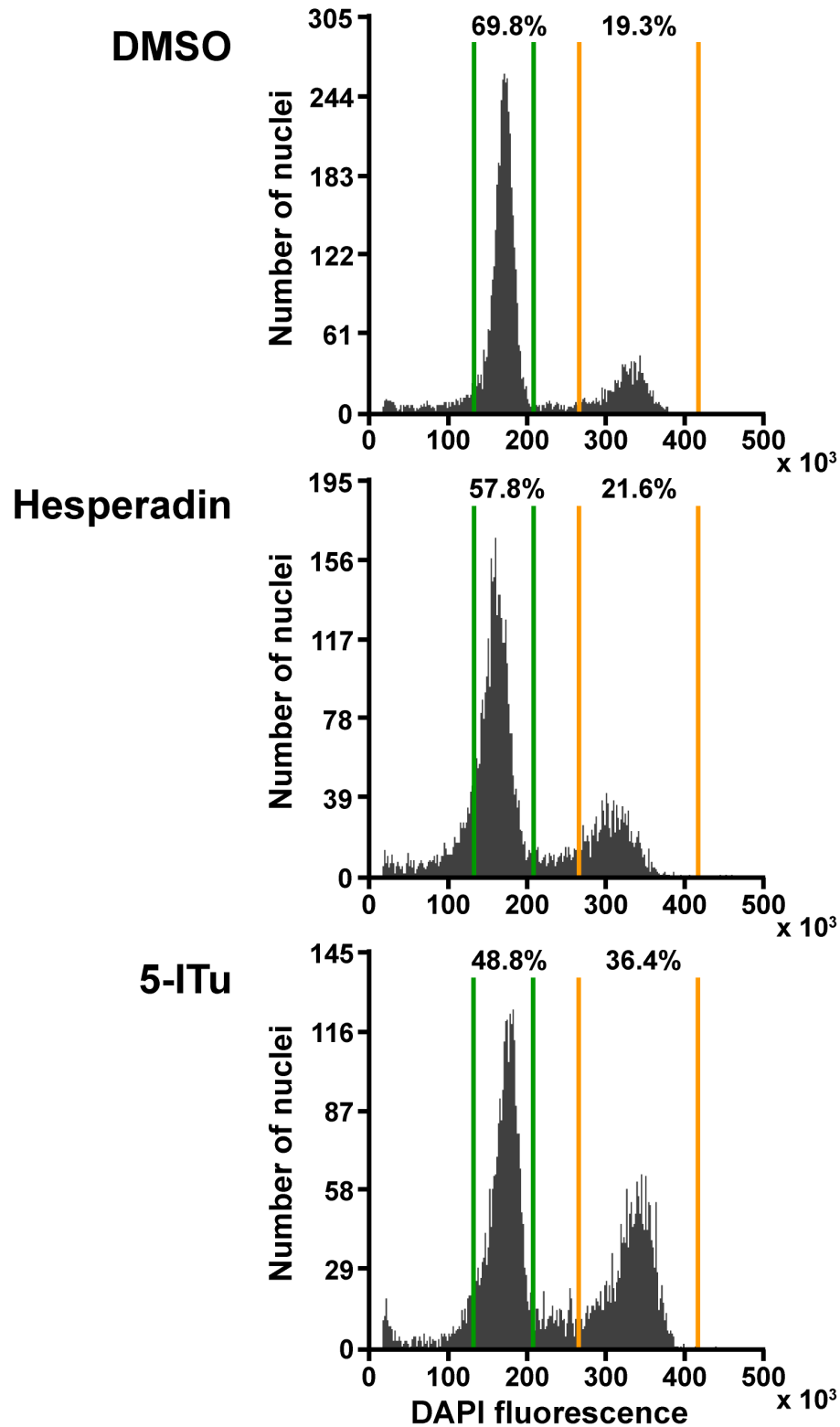
Supplementary Figure S2. Distribution of NtAUR2 through the cell cycle.

Live-cell imaging was performed in BY-2 cells expressing NtAUR2-mClover after 1-h treatment with DMSO as a control (A) or 1 μ M 5-ITu (B). Images are maximum projections of z-stack. Scale bar = 10 μ m.



Supplementary Figure S3. Cell plate expansion rate.

Data was acquired from live-cell imaging in BY-2 cells expressing GFP-KNOLLE. Live-imaging was performed after 1-h treatment with DMSO, 2 μ M LatB or 1 μ M 5-ITu and images were acquired every 5 min. Every time point shows mean value of the cell plate diameter \pm SD, for \geq 17 mitotic cells in each concentration.



Supplementary Figure S4. Analysis of cell culture ploidy.

Cell treated for 24-h with DMSO, 5 μ M Hesperadin or 1 μ M 5-ITu were analyzed by flow cytometry.

First peak (in green lines) corresponds to 2C nuclei; second peak (in yellow lines) corresponds to 4C nuclei. Typical data from at least five independent measurements is shown.

Supplementary Movie S1. Live-imaging of NtAUR3 distribution throughout the cell cycle.

Live-cell imaging was performed on BY-2 cells expressing NtAUR3-mClover after a 1-h treatment with DMSO (control). Scale bar = 10 μm .

Supplementary Movie S2. Live-imaging of NtAUR3 under 5-ITu treatment.

Live-cell imaging was performed on BY-2 cells expressing NtAUR3-mClover after a 1-h treatment with 1 μM 5-ITu. Scale bar = 10 μm .

Supplementary Movie S3. Spindle assembly checkpoint transition under 5-ITu treatment.

Live-cell imaging was performed on BY-2 cells expressing tdTomato-cenH3 after a 1-h treatment with 1 μM 5-ITu. Scale bar = 10 μm .

Supplementary Table S1. The list of primers in this study.